Chapter 8

BEAM LOADING AND ROBINSON'S STABILITY

Klystron or tetrodes* are employed to drive the rf cavities. When a klystron or tetrode is coupled to an rf cavity, electromagnetic fields are generated inside the cavity. The electric field across the gap of the cavity provides the required power to compensate for the energy loss to synchrotron radiation and coupling impedance, and to supply the necessary acceleration to the particle beam. However, the particle beam, when passing through the gap of the rf cavity, also excites electromagnetic fields inside the cavity in the same way as the klystron or the rf source. This excitation of the cavity by the particle beam is called *beam loading*. Beam loading has two effects on the rf system. First, the electric field from beam loading generates a potential, called the *beam loading voltage*, across the cavity gap and opposes the accelerating voltage delivered by the klystron. Thus more power has to be supplied to the rf cavity in order to overcome the effect of beam loading. Second, to optimize the power of the klystron, the cavity needs to be detuned. The detuning has to be performed correctly. If not, the power delivered by the klystron will not be efficient. Worst of all, an incorrect detuning will excite instability of the phase oscillation. We first study the steady-state beam loading and derive the criterion for phase stability. Later, transient beam loading will be addressed. The general methods to suppress beam loading are also reviewed. Most of the material in this chapter comes from the lecture notes of Wilson [1], Wiedemann [2], and Boussard [3].

---

*Klystrons are usually used in electron rings where the rf frequencies are high while tetrodes are usually used in proton rings where the rf frequencies are low. In this chapter, there is no intention to distinguish between the two, and we often use the terminology *rf generator* instead.
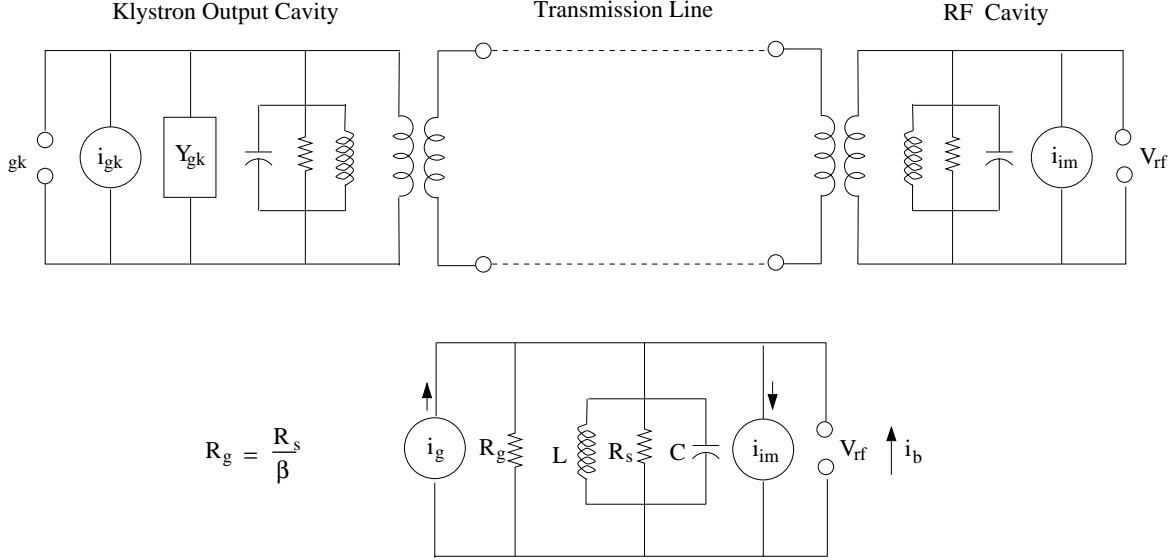
8.1   Equivalent Circuit

Figure 8.1: Circuit model representing an rf generator current source i_g driving an rf cavity with a beam loading current i_{im}.

The rf system can be represented by an equivalent circuit as shown in the top diagram of Fig. 8.1. The rf cavity is represented by a RLC circuit with angular resonant frequency

$$\omega_r = \frac{1}{\sqrt{LC}} \; , \tag{8.1}$$

where L and C are the equivalent inductance and capacitance of the rf cavity. The klystron or tetrode is also represented by a RLC circuit with the angular resonant frequency $\omega_{\rm rf}$, which is the actual rf frequency of the accelerator ring. The klystron/tetrode is connected to the rf cavity by waveguides or transmission lines via transformers as illustrated. The problem can be simplified considerably by assuming that there is a circulator or isolator just before the rf cavity, so that any power which is reflected from the cavity and travels back towards the klystron will be absorbed. Such an assumption leads to the equivalent circuit in the lower diagram of Fig. 8.1. The resistor R_s is called the *unloaded shunt impedance* of the rf system, because it is the impedance of the isolated cavity at its resonant frequency. The image current of the particle beam is represented by a current source i_{im}. This is a valid representation from the rigid-bunch approximation, because the velocities and therefore the current of the beam particles are assumed

roughly constant when the beam passes through the cavity gap. We reference image current here instead of the beam current i_b, because it is the image current that flows across the cavity gap and also into the cavity. The image current is in opposite direction to the beam current.

On the other hand, the situation is different for the klystron. The velocities of the electrons as they pass through the the gap of the output cavity of the klystron can change in response to the cavity fields of the klystron. As a consequence, the rf source is represented by a current source i_g in parallel to the loading resistor R_g or admittance $Y_g = 1/R_g$. The latter is written in terms of the shunt admittance Y_s or shunt impedance R_s of the rf cavity as

$$Y_g = \beta Y_s = \frac{\beta}{R_s} \; , \tag{8.2}$$

where β is the *coupling coefficient* still to be defined. The generator or klystron current i_g and the loading admittance Y_g in the lower equivalent circuit diagram are equivalent values and are different from the actual generator current i_{gk} and actual loading admittance Y_{gk} in the klystron circuit in the top circuit of Fig. 8.1. For example, in the rf system of the Fermilab Main Injector, $i_{gk} = 12i_g$.

The rf generator outputs a generator current I_g in order to produce the rf gap voltage $V_{\rm rf}$ for the beam. The total *required* output power[†] is

$$P_{\rm total} = \frac{1}{2} \frac{I_g^2}{Y_g + Y_{\rm load}} \; , \tag{8.3}$$

where $Y_{\rm load}$ is called the *load cavity admittance*, which includes the admittance of the cavity $Y_s = 1/R_s$ and also all the contribution from the particle beam. An explicit expression will be given in Eq. (8.43) below. In the situation of a very weak beam $(i_b \to 0)$, $Y_{\rm load} \to Y_s$. The total power can be rewritten as

$$P_{\rm total} = \frac{1}{2} \frac{Y_g I_g^2}{(Y_g + Y_{\rm load})^2} + \frac{1}{2} \frac{Y_{\rm load} I_g^2}{(Y_g + Y_{\rm load})^2} \; . \tag{8.4}$$

The first term on the right is the power dissipated at the generator. The second term is the power required to be transferred to the cavity and the beam, and we denote it

---

[†]This is the power *required* to transfer a certain energy per unit time to the cavity and the beam, and is different from the power available to the beam and cavity. The latter is given by $\frac{1}{2}\tilde{I}_g \cdot \tilde{V}_{\rm rf}$ and becomes zero when the load angle $\theta_L = \pi/2$, as indicated in Eq. (8.38). On the other hand, the required power is inversely proportional to $\cos^2 \theta_L$. When $\theta_L \to \pi/2$, most of the energy energy is being transferred to the cavity as stored energy and very little is given to the beam. Therefore to satisfy the requirement of the beam, an infinite required power by the generator becomes necessary.

by P_g, which is usually referred to loosely as the *generator power*. We wish to obtain the condition for which this power delivered to the cavity and beam is a maximum by equating its derivative with respect to Y_{load} to zero. The condition is

$$Y_{\text{load}} = Y_g = \beta Y_s \ . \tag{8.5}$$

This is just the usual matching of the input impedance to the output impedance. The maximized generator power is then

$$P_g = \frac{i_g^2}{8\beta Y_s} = \frac{R_s i_g^2}{8\beta} \ . \tag{8.6}$$

Notice that in the situation of an extremely weak beam, this matched condition is just $Y_g = Y_s$ with the coupling coefficient $\beta = 1$. Equation (8.6) will be used repeatedly below and whenever the generator power P_g is referenced, we always imply the matched condition satisfying Eq. (8.5).

Here, all the currents and voltages referenced are the magnitudes of sinusoidally varying currents and voltages at the rf angular frequency ω_{rf} (not the cavity resonant angular frequency ω_r). Their corresponding phasors always have an overhead tilde. For example, i_{im} is the magnitude of the Fourier component of the image current phasor $\tilde{i}_m$ that flows into the cavity at the rf frequency. Thus, for a *short bunch*, we have (Exercise 8.1),

$$i_{im} = 2I_0 \ , \tag{8.7}$$

with I_0 being the *dc current* of the beam. As phasors, however, they are in the opposite direction. It will be shown later, the image current phasor $\tilde{i}_m$ may not be equal to the negative beam current phasor $\tilde{i}_b$ because of possible feed-forward. In that case, I_0 in Eq. (8.7) will be the dc image current instead. For this reason, we try to make reference to the image current that actually flows into the cavity instead of the beam current.

In high energy electron linacs, bunches are usually accelerated at the peak or crest of the rf voltage wave in order to achieve maximum possible energy gain. As a result, the klystron is operated at exactly the same frequency as the resonant frequency of the rf cavities, i.e., $\omega_{\text{rf}} = \omega_r$. Without the rf generator, the beam or image current sees the *unloaded shunt impedance* R_s in the cavity and the *unloaded quality factor* Q_0, which can easily be found to be

$$Q_0 = \omega_r C R_s \ . \tag{8.8}$$

With the rf generator attached, however, the beam image current source sees an effective shunt impedance R_L in the cavity, which is the parallel combination of the generator

shunt impedance R_g and the cavity shunt impedance R_s. This is called the cavity *loaded shunt impedance* in contrast with the cavity unloaded shunt impedance R_s. We therefore have

$$R_L = (Y_s + Y_g)^{-1} = \frac{R_s}{1 + \beta} \ . \tag{8.9}$$

Correspondingly, the beam image current sees a *loaded quality factor* in the cavity, which is

$$Q_L = \omega_r C R_L = \frac{Q_0}{1 + \beta} \ . \tag{8.10}$$

Notice that

$$\frac{R_s}{Q_0} = \frac{R_L}{Q_L} \ , \tag{8.11}$$

independent of whether it is loaded or unloaded. In fact, R_s/Q_0 is just a geometric factor of the cavity.

The beam loading voltage is the voltage generated by the image current, and is given by

$$V_{br} = \frac{i_{im}}{Y_g + Y_s} = \frac{i_{im}}{Y_s(1 + \beta)} \ , \tag{8.12}$$

while the voltage produced by the generator is

$$V_{gr} = \frac{i_g}{Y_g + Y_s} = \frac{i_g}{Y_s(1 + \beta)} \ , \tag{8.13}$$

where the subscript "r" implies that the operation is at the resonant frequency, so that the currents and voltages are in phase, although they may have sign difference. In terms of the generator power P_g in Eq. (8.6), the generator voltage at resonance becomes

$$V_{gr} = \frac{\sqrt{8\beta}}{1 + \beta} \sqrt{R_s P_g} \ . \tag{8.14}$$

It is clear that the beam loading voltage is in the opposite direction of the generator voltage. Thus, the net accelerating voltage is

$$V_{\mathrm{rf}} = V_{gr} - V_{br} = \sqrt{R_s P_g} \left[\frac{\sqrt{8\beta}}{1 + \beta} \left(1 - \frac{K}{2\sqrt{\beta}} \right) \right] \ , \tag{8.15}$$

where

$$K^2 = \frac{i_{im}^2 R_s}{2P_g} \tag{8.16}$$

plays the role of the ratio of the beam loading power to the generator power. Since the shunt impedance R_s of a superconducting cavity is very high, beam loading becomes much more important. The fraction of generator power delivered to the beam is

$$\eta = \frac{i_{im}V_{\text{rf}}}{2P_g} = \frac{2\sqrt{\beta}}{1+\beta}K\left(1 - \frac{K}{2\sqrt{\beta}}\right) \ . \tag{8.17}$$

The power dissipated in the cavity is

$$P_c = \frac{V_{\text{rf}}^2}{2R_s} = P_g\left(\frac{2\sqrt{\beta}}{1+\beta}\right)^2\left(1 - \frac{K}{2\sqrt{\beta}}\right)^2 \ . \tag{8.18}$$

From the conservation of energy, we must have

$$P_g = \eta P_g + P_c + P_r \ , \tag{8.19}$$

where P_r is the power reflected back to the generator and is given by

$$\frac{P_r}{P_g} = \left(\frac{\beta - 1 - K\sqrt{\beta}}{1+\beta}\right)^2 \ . \tag{8.20}$$

So far we have not said anything about the coupling coefficient β. Now we can choose β so that the generator power is delivered to the cavity and the beam without any reflection, or from Eq. (8.20), the optimum coupling constant is

$$K = \frac{\beta_{\text{op}} - 1}{\sqrt{\beta_{\text{op}}}} \ . \tag{8.21}$$

Notice that this optimization is also a maximization of the accelerating voltage V_{rf}, as can be verified by differentiating Eq. (8.15) with respect to β.

8.2   Beam Loading in an Accelerator Ring

In a synchrotron ring or storage ring, it is necessary to operate the rf system off the crest of the accelerating voltage wave form in order to have a sufficient large bucket area to hold the bunched beam and to insure stability of phase oscillation. The klystron or rf generator is operating at the *rf frequency* $\omega_{\text{rf}}/(2\pi) = h\omega_0/(2\pi)$, where h is an integer called the *rf harmonic*, and $\omega_0/(2\pi)$ is the revolution frequency of the *synchronized* beam particles. Notice that this rf frequency will be the frequency the beam particles

experience at the cavity gap and is different from the intrinsic resonant frequency of the cavity $\omega_r/(2\pi)$ given by Eq. (8.1). According to the circuit diagram of Fig. 8.1, the impedance of the cavity seen by the particle at rf frequency $\omega_{\rm rf}/(2\pi)$ can be written as

$$Z_{\rm cav} = \frac{R_L}{1 - jQ_L\left(\dfrac{\omega_r}{\omega_{\rm rf}} - \dfrac{\omega_{\rm rf}}{\omega_r}\right)} = R_L \cos\psi\, e^{j\psi} \ , \tag{8.22}$$

where ψ is called the *rf detuning angle* or just detuning. As will be shown below, detuning is an essential mechanism to make the beam particle motion stable under the influence of the rf system. It is important to point out that loaded values have been used here, because those are what the image current sees. From Eq. (8.22), the detuning angle is defined as

$$\tan\psi = Q_L\left(\frac{\omega_r}{\omega_{\rm rf}} - \frac{\omega_{\rm rf}}{\omega_r}\right) \ . \tag{8.23}$$

When the deviation of $\omega_{\rm rf}$ from ω_r is small, an approximation gives

$$\tan\psi = 2\,Q_L\frac{\omega_r - \omega_{\rm rf}}{\omega_r} \ . \tag{8.24}$$

Note that in this section we have used j instead of $-i$, because phasor diagrams are customarily drawn using this convention. Phasors, as illustrated in Fig. 8.2, are represented by overhead tildes rotating counter-clockwise with angular frequency $\omega_{\rm rf}$ if there is only one bunch in the ring. If there are N_b equal bunches in the ring separated equally by $h_b = h/N_b$ rf buckets, where h is the rf harmonic, we can also imagine the phasors to be rotating at angular frequency $\omega_{\rm rf}/h_b$. They are therefore the Fourier components at the rf frequency or $\omega_{\rm rf}/h_b$. This implies that we are going to see the same phasor plot for each passage of a bunch through the rf cavity. In order to be so, the beam loading voltage should have negligible decay during the time interval $T_b = 2\pi h_b/\omega_{\rm rf}$ between two successive bunches. In other words, we require $T_b \ll T_f$ in this discussion, where $T_f = 2Q_L/\omega_r$ is the fill time of the cavity.

Most of the time, the image current phasor $\tilde{i}_{\rm im}$ has the same magnitude as that of the beam current phasor $\tilde{i}_b$, although in the opposite direction. When the image current $\tilde{i}_{\rm im}$ interacts with the loaded cavity, according to Eq. (8.22), a beam loading voltage phasor $\tilde{V}_b$ will be produced and is given by

$$\tilde{V}_b = \tilde{i}_{\rm im}R_L \cos\psi e^{j\psi} \ , \tag{8.25}$$
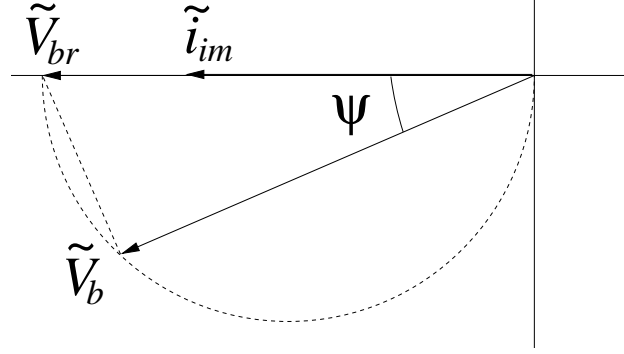
and

$$V_b = V_{br}\cos\psi \ . \tag{8.26}$$

Figure 8.2: Phasor plot showing the beam loading voltage phasor $\tilde{V}_b$ induced in the rf cavity by the image current phasor $\tilde{i}_{im}$, which lags $\tilde{V}_b$ by the detuning angle ψ. Also plotted is the beam loading voltage phasor $\tilde{V}_{br}$, with $V_b = V_{br}\cos\psi$ when the beam current is at the crest of the rf wave with no detuning.

Thus the voltage phasor always leads the current phasor by the detuning phase ψ and the magnitude of the phasor $\tilde{V}_b$ is less than its value at the cavity resonant frequency V_{br} by the factor $\cos\psi$. If one likes, one can also introduce the phasor $\tilde{V}_{br}$ which is in phase with the current phasor $\tilde{i}_{\mathrm{im}}$ and has the magnitude given by Eq. (8.26). This is illustrated in Fig. 8.2.

Some comments are necessary. Here, we start from only one Fourier component (the one at frequency ω_{rf} or ω_{rf}/h_b) of the image current $\tilde{i}_{\mathrm{im}}$. The beam loading voltage $\tilde{V}_b$ experienced by the beam is also a Fourier component of the same frequency. Since we are investigating the problem in the frequency domain, this is equivalent to a very long interval in the time domain. In other words, the result describes a steady-state problem, implying that the beam has passed by the rf cavities many many times already. The beam loading voltage $\tilde{V}_b$ is therefore a sinusoidal wave in time. However, this is not exactly what we expect from a cavity. The beam loading voltage decays exponentially as soon as the beam leaves the rf cavity. It is charged up again like a step function when the beam passes by again. Thus, the time dependent behavior of the beam loading voltage is more like a sawtooth rather than sinusoidal. Putting it in another way, more than one Fourier component will be necessary to fully describe the beam loading picture. However, if the exponential decay is slow, the beam loading wave will behave more like sinusoidal. Therefore, our description of the beam loading problem here is valid only when the cavity decay time constant (or fill time)

$$T_f = \frac{2Q_L}{\omega_r} \tag{8.27}$$

is very much longer than the interval T_b between successive beam passage. We will address a more accurate description later.

There are good reasons that detuning is necessary. The first one is for the compensation of beam loading, which we describe in the next subsection. One may argue why we do not just employ an extra generator current equal and opposite to the image current for a simple 100% compensation. This requires the generator to deliver unnecessarily large current at a phase angle other than that of the rf voltage. Needless to say, this will result in a degradation of the efficiency of the rf excitation system and an increase in cost. The second reason is phase stability. When the center of the beam deviates from its proper rf phase, proper detuning will damp the deviation and guarantee phase stability. This will be addressed later in the section on Robinson's stability.

8.2.1   Steady-State Compensation

In Fig. 8.3, the total current phasor $\tilde{i}_t$ inside the cavity is the vector sum of the image current phasor $\tilde{i}_{\rm im}$ and the generator current phasor $\tilde{i}_g$. The rf voltage phasor $\tilde{V}_{\rm rf}$ is at the synchronous angle ϕ_s and leads the total current phasor by the detuning angle ψ. The current phasor $\tilde{i}_0$ is the projection of $\tilde{i}_t$ along $\tilde{V}_{\rm rf}$. Thus, $\tilde{i}_0$ is the generator current required to set up the rf voltage when the cavity is at resonance and when there is no beam current. In other words, $i_0 = V_{\rm rf}/R_L = (1 + \beta)V_{\rm rf}/R_s$, where β is the coupling coefficient of the generator to the rf cavity and R_s is the unloaded shunt impedance.

We want to solve for the *load angle* θ_L that the the generator current phasor lags the rf voltage phasor. By projecting along and perpendicular to the rf voltage phasor, one obtains

$$\tan \theta_L = \frac{i_0 \tan \psi - i_{\rm im} \cos \phi_s}{i_0 + i_{\rm im} \sin \phi_s} \; , \tag{8.28}$$

and

$$i_g = \frac{i_0 + i_{\rm im} \sin \phi_s}{\cos \psi} \; . \tag{8.29}$$

To optimize the efficiency of the generator, the generator current phasor $\tilde{i}_g$ and the rf voltage phasor $\tilde{V}_{\rm rf}$ should be in the same direction, because in this way the load will appear real to the generator and the stored energy will be reduced to a minimum.
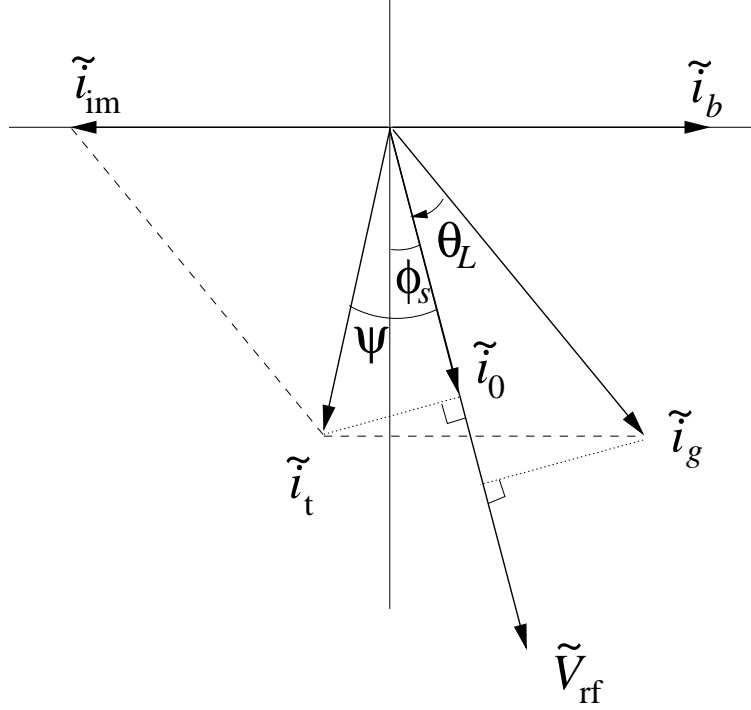
Figure 8.3: Phasor plot showing the vector addition of the image current phasor $\tilde{i}_{\mathrm{im}}$ and the generator current phasor $\tilde{i}_g$ to give the total current phasor $\tilde{i}_t$. The latter lags the rf voltage phasor $\tilde{V}_{\mathrm{rf}}$ at synchronous phase ϕ_s by the detuning angle ψ. Note that the generator current phasor is not in phase with the rf voltage phasor. It lags $\tilde{V}_{\mathrm{rf}}$ by the load angle θ_L.

Substituting for $\theta_L = 0$, we obtain the in-phase conditions

$$\tan \psi = \frac{i_{im} \cos \phi_s}{i_0} \tag{8.30}$$

and

$$i_g = i_0 + i_{\mathrm{im}} \sin \phi_s \ . \tag{8.31}$$

Figure 8.4 shows the voltage phasors inside the cavity with the rf voltage phasor $\tilde{V}_{\mathrm{rf}}$ in phase with the generator current phasor $\tilde{i}_g$. Here, we see that the beam loading voltage phasor $\tilde{V}_b$ is ahead of the image current phasor $\tilde{i}_{\mathrm{im}}$ by the detuning angle ψ. The generator voltage phasor $\tilde{V}_g$ is also ahead of the generator current phasor $\tilde{i}_g$ by the detuning angle ψ. These two voltage phasors add up to give the gap voltage phasor $\tilde{V}_{\mathrm{rf}}$ which has a synchronous angle ϕ_s. The in-phase condition can also be obtained from this phasor diagram. Since the voltage components perpendicular to $\tilde{i}_g$ must add up to
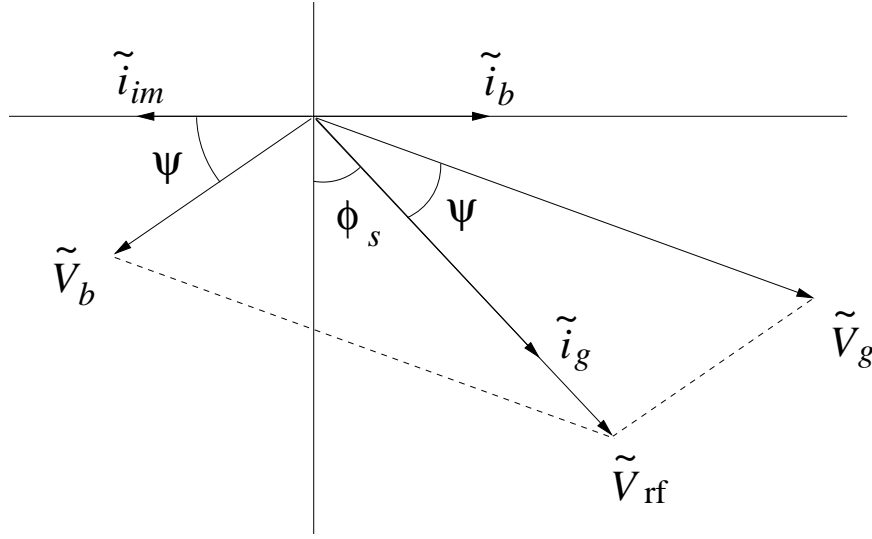
Figure 8.4: Phasor plot showing the vector addition of the generator voltage phasor $\tilde{V}_g$ and the beam loading voltage phasor $\tilde{V}_b$ to give the gap voltage phasor $\tilde{V}_{\rm rf}$ in an rf cavity. Note the detuning angle ψ which puts the gap current phasor $\tilde{i}_g$ in phase with the gap voltage phasor.

zero, after dividing by $R_s \cos\psi$, we get

$$i_g \sin\psi = i_{\rm im} \sin\left(\tfrac{\pi}{2} + \phi_s - \psi\right) . \tag{8.32}$$

Next, resolve the current contributions along $\tilde{i}_g$ and we obtain Eq. (8.31). Finally, eliminate i_g and arrive at the in-phase condition of Eq. (8.30).

Notice that steady-state beam loading has been compensated by the introduction of a suitable generator current. This compensation scheme with detuning is much more efficient than the one without, because part of the beam loading voltage has been utilized in the rf voltage and the generator current is in phase with the rf voltage. In other words, the generator power required will be smaller than when there is no detuning. Actually, it can be readily shown by differentiating Eq. (8.35) below with respect to the detuning angle ψ that the generator power is the smallest when the in-phase condition is met between the generator current phasor and the rf voltage phasor. In the event that the beam intensity is very high, the beam loading voltage V_b can become much larger than the required gap voltage $V_{\rm rf}$. Needless to say, to balance such a large a very high power amplifier will be necessary to generate the required generator current I_g. When this happens, low-level rf feedback can be installed to reduce the effective cavity impedance as observed by the beam. A low-level rf feed-forward is also possible to cancel partly or

completely the image current. These methods will be discussed later in Sec. 8.4.4.

The generator power P_g can be computed with the aid of Eq. (8.14), namely,

$$P_g = \frac{(1+\beta)^2 V_{gr}^2}{8\beta R_s} , \tag{8.33}$$

where V_{gr} is the generator voltage at the cavity resonant frequency, and is related to the generator voltage V_g at the rf frequency by $V_g = V_{gr}\cos\psi$. Using the cosine law for the triangle made up from $\tilde{V}_g$, $\tilde{V}_b$, and $\tilde{V}_{\rm rf}$, it is easy to obtain

$$V_g^2 = V_b^2 + V_{\rm rf}^2 - 2V_b V_{\rm rf}\sin(\psi - \phi_s) , \tag{8.34}$$

or

$$V_{gr}^2 = V_{br}^2 + V_{\rm rf}^2(1 + \tan^2\psi) - 2V_{br}V_{\rm rf}(\tan\psi\cos\phi_s - \sin\phi_s) , \tag{8.35}$$

where $V_{br} = V_b/\cos\psi$ is the beam loading voltage at the cavity resonant frequency. From Eq. (8.14), the required generator power for the cavity and beam can be expressed as

$$P_g = \frac{R_s}{8\beta}\left[(i_0 + i_{\rm im}\sin\phi_s)^2 + (i_0\tan\psi - i_{\rm im}\cos\phi_s)^2\right] , \tag{8.36}$$

where

$$V_{br} = \frac{V_b}{\cos\psi} = \frac{i_{\rm im}R_s}{1+\beta} \tag{8.37}$$

is the beam loading voltage at the cavity resonant frequency, and the definition of i_0 in Eq. (8.31) has been used. If the correct detuning is made so that $\tilde{I}_g$ and $\tilde{V}_{\rm rf}$ are in phase, the second term on the right-hand side vanishes and the expression is very much simplified. On the other hand, we notice that the two terms on the right-side resemble the denominator and numerator on the right-side of Eq. (8.28). We can therefore rewrite the generator power in terms of the load angle θ_L,

$$P_g = \frac{R_s}{8\beta}\frac{(i_0 + i_{\rm im}\sin\phi_s)^2}{\cos^2\theta_L} , \tag{8.38}$$

which recovers the situation of in-phase detuning when $\theta_L = 0$. The factor $\cos^2\theta_L$ is important. It tells us that when the load angle $\theta_L \to \pi/2$, an infinite generator power is required. This is because only the fraction $\cos^2\theta_L$ of the power goes into the beam and the majority, $\sin^2\theta_L$, goes into charging the cavity.

Again we can optimize the generator power by choosing the best coupling constant β, which turns out to be

$$\beta_{\rm op} = 1 + \frac{i_{\rm im}R_s\sin\phi_s}{V_{\rm rf}} = 1 + \frac{P_b}{P_c} , \tag{8.39}$$

where

$$P_c = \frac{V_{\text{rf}}^2}{2R_s} \tag{8.40}$$

is the power dissipated in the walls of the cavity and

$$P_b = \tfrac{1}{2}\, i_{im} V_{\text{rf}} \sin\phi_s = I_0 V_{\text{rf}} \sin\phi_s \tag{8.41}$$

is the power spent on accelerating the beam, since $V_{\text{rf}} \sin\phi_s$ is the accelerating voltage. Here, we have used Eq. (8.7), the fact that the Fourier component image current at the rf frequency (or at ω_{rf}/h_b) is nearly twice the dc beam current I_0 when the bunch is short. At the optimized coupling constant, the generator power becomes

$$P_{g\,\text{op}} = \frac{V_{\text{rf}}^2}{2R_g} = \frac{V_{\text{rf}}^2}{2R_s}\,\beta_{\text{op}} = P_b + P_c\ , \tag{8.42}$$

which just states that the power is transmitted to the cavity completely without any reflected. Here, we can identify the *load cavity admittance* Y_{load} defined in earlier in Eq. (8.4) as

$$Y_{\text{load}} = \frac{i_{\text{im}} \sin\phi_s}{V_{\text{rf}}} + \frac{1}{R_s}\ , \tag{8.43}$$

where the first term on the right is admittance of the beam and the second term is the admittance of the cavity.

Usually there is a servo-tuner which measures the phase difference between the generator current phasor and rf gap voltage phasor, and controls the cavity tune via a mechanical plunger or ferrite bias, so that the phase difference vanishes. At equilibrium of the servo-tuner, Eqs. (8.30) and (8.31) are automatically satisfied, and the cavity detuning corresponds to

$$\Delta\omega = \omega_r - \omega_{\text{rf}} = \frac{\omega_r R_L i_{\text{im}} \cos\phi_s}{2Q_L V_{\text{rf}}}\ . \tag{8.44}$$

8.3   Robinson's Stability Criteria

8.3.1   Phase Stability at Low Intensity

We are now in the position to discuss the conditions for phase stability. Suppose that center of the bunch has the same energy as the synchronous particle, but is at a small
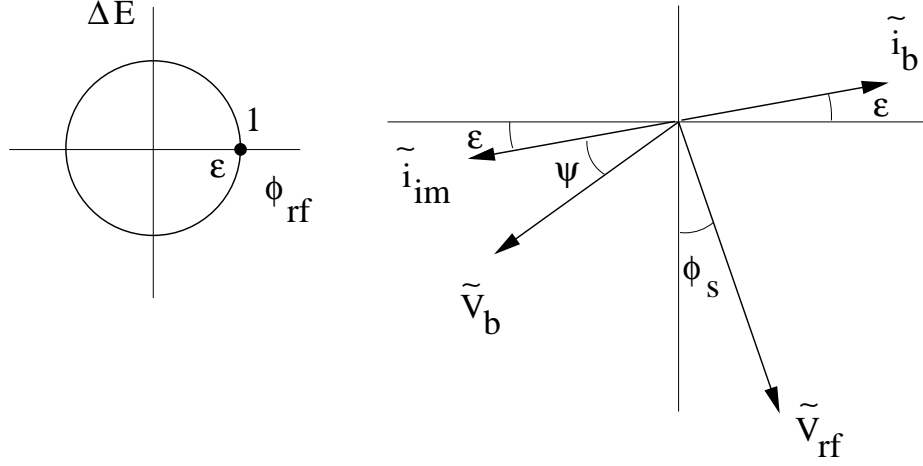
Figure 8.5: With the bunch center at Point 1 in the synchrotron oscillation, the beam current phasor $\tilde{i}_b$ arrives earlier by being ahead of the x-axis at a small angle $\epsilon > 0$ in the phasor plot. The bunch sees a smaller rf voltage $V_{\rm rf}\sin(\phi_s - \epsilon)$ if the synchronous phase $0 < \phi_s < \frac{1}{2}\pi$. It is decelerated. Below transition, it will arrive not so early in the next turn and phase stability is therefore established.

phase advance $\phi_{\rm rf} = \epsilon > 0$, as depicted by Point 1 in the synchrotron oscillation and the phasor $\tilde{i}_b$ in the phasor plot in Fig. 8.5. The phasor $\tilde{i}_b$ arrives earlier by being ahead of the x-axis at a small angle $\epsilon > 0$. Then the accelerating voltage it sees will be $V_{\rm rf}\sin(\phi_s - \epsilon)$ instead of $V_{\rm rf}\sin\phi_s$, or an extra decelerating voltage of $\epsilon V_{\rm rf}\cos\phi_s$ if $0 < \phi_s < \frac{1}{2}\pi$. Receiving less energy from the rf voltage than the synchronous particle will slow the bunch. If the beam is below transition, this implies the reduction of its revolution frequency, so that after the next h rf periods its arrival ahead of the synchronous particle will be smaller or ϵ will become smaller. The motion is therefore stable. Therefore to establish stable phase oscillation when beam loading can be neglected, one requires

$$\begin{cases} 0 < \phi_s < \frac{\pi}{2} & \text{below transition,} \\ \frac{\pi}{2} < \phi_s < \pi & \text{above transition.} \end{cases} \tag{8.45}$$

This is exactly the same condition for stable phase oscillation we conclude from the expression for the synchrotron tune in Eq. (2.14). Notice that this is just the condition of phase stability and there is no damping at all. Here, the derivation relies on the fact that the rf voltage phasor $\tilde{V}_{\rm rf}$ is unperturbed and this is approximately correct when the beam intensity and therefore the beam loading voltage is small.

8.3.2   Phase Stability at High Intensity

When the beam current is very intense, we can no longer neglect the contribution of the beam loading voltage. The condition of phase stability in Eq. (8.45) will be modified. Now, go back to Fig. 8.5 when the beam current phasor arrives at an angle $\epsilon > 0$ ahead of the x-axis but is at the same energy as the synchronous particle, the image current phasor $\tilde{i}_{\mathrm{im}}$ will also advance by the same angle ϵ after h rf periods. Therefore, there will be an extra beam loading voltage phasor $\epsilon i_{\mathrm{im}} R_L \cos\psi\, e^{j(\psi+3\pi/2)}$, which constitutes the perturbation of the rf voltage phasor $\tilde{V}_{\mathrm{rf}}$. If $\psi < 0$, this phasor will point into the 3rd quadrant and decelerate the particle in concert with $\epsilon V_{\mathrm{rf}} \cos\phi_s$ in slowing the beam, thus causing no instability below transition. On the other hand, if $\psi > 0$, this phasor will point into the 4th quadrant and accelerate the particle instead. To be stable, the extra accelerating voltage on the beam must be less than the amount of decelerating voltage $\epsilon V_{\mathrm{rf}} \cos\phi_s$, or

$$\left[V_{\mathrm{rf}} \sin(\phi_s - \epsilon) - V_{\mathrm{rf}} \sin\phi_s \right] + \epsilon i_{\mathrm{im}} R_L \cos\psi \sin\psi \approx -\epsilon V_{\mathrm{rf}} \cos\phi_s + \epsilon V_{br} \cos\psi \sin\psi < 0 \ . \tag{8.46}$$

Thus for phase stability, we require

$$\frac{V_{br}}{V_{\mathrm{rf}}} < \frac{\cos\phi_s}{\sin\psi \cos\psi} \qquad \begin{cases} \psi > 0 & \text{below transition,} \\ \psi < 0 & \text{above transition,} \end{cases} \tag{8.47}$$

which is called Robinson's *high-intensity criterion* of stability. In above, $V_{br} = i_{\mathrm{im}} R_L$ is the *in-phase* beam loading voltage when the beam is in phase with the loaded cavity impedance.

Notice that this Robinson's high-intensity criterion of stability is only a criterion of phase stability similar to the phase stability condition of Eq. (8.45). Satisfying this criterion just enables stable oscillating like sitting inside a stable potential well. Violating this criterion will place the particle in an unstable potential well so that phase oscillation will not be possible. To include damping or antidamping due to the interaction of the beam with the cavity impedance, another criterion of Robinson stability, Eq. (8.57) below, must be satisfied also.

We can also look at the phase stability problem in another way. In order that the beam can execute stable phase oscillation, it must see a linear restoring force when the beam deviates from its equilibrium position. This force comes from change in the rf voltage $\tilde{V}_{\mathrm{rf}}$ seen by the beam when the beam is at an offset. This explains why we have
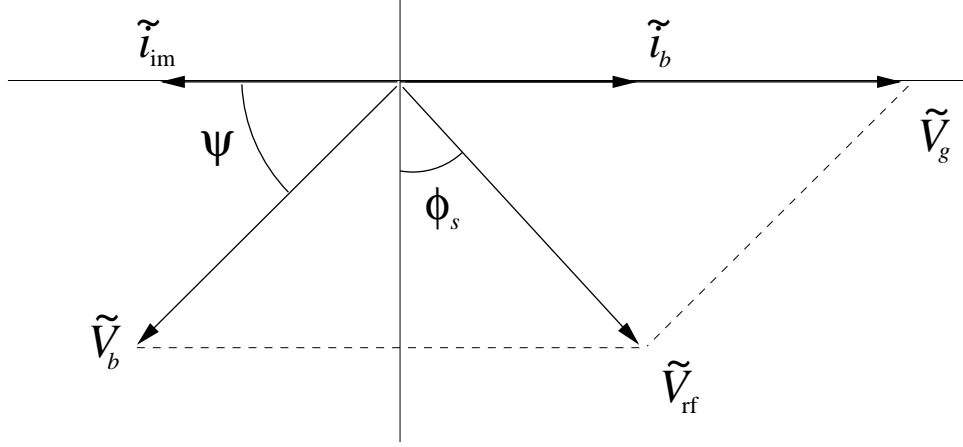
Figure 8.6: When the generator voltage phasor $\tilde{V}_g$ becomes in phase with the beam current phasor, it provides no force gradient to the beam in the direction of the beam. Since the restoring force vanishes for an infinitesimal offset of the beam arrival time, the beam is on the edge of instability in phase oscillation.

the gradient of the rf accelerating voltage or $V_{\mathrm{rf}} \cos \phi_s$ in Eq. (2.14), the expression of the synchrotron tune. Now the rf voltage phasor $\tilde{V}_{\mathrm{rf}}$ is the sum of the beam loading voltage phasor $\tilde{V}_b$ and the generator voltage phasor $\tilde{V}_g$, or

$$\tilde{V}_{\mathrm{rf}} = \tilde{V}_b + \tilde{V}_g \ . \tag{8.48}$$

Notice that the beam loading voltage phasor $\tilde{V}_b$ moves with the beam and therefore will not provide any force gradient or restoring force to the beam. In other words, $d\tilde{V}_b/d\epsilon = 0$. Thus only the generator voltage phasor $\tilde{V}_g$ can provide such a restoring force. Therefore, we should compute $d\tilde{V}_g/d\epsilon$. If this gradient enhances the displacement of the beam from the synchronous position, the system is unstable; otherwise, it is stable. When the generator voltage phasor is in phase with the beam as illustrated in Fig. 8.6, it is clear that for any small variation of time arrival ϵ of the beam, the beam will not see any variation of the generator voltage phasor $\tilde{V}_g$ in the direction of the beam, or $d\tilde{V}_g/d\epsilon = 0$ in the direction of the beam. In other words, there is no restoring force to alter the energy of the beam so as to push it back to its equilibrium position. Thus the configuration in Fig. 8.6 constitutes the Robinson's limit of phase stability. From the figure, it is evident that the projection of $\tilde{V}_{\mathrm{rf}}$ and $\tilde{V}_b$ perpendicular to the beam must be the same or the stability limit is

$$V_{\mathrm{rf}} \cos \phi_s = i_{\mathrm{im}} R_L \cos \psi \sin \psi \ , \tag{8.49}$$

which is exactly the same as Eq. (8.47).

Now let us impose the condition that the generator current $\tilde{i}_g$ is in phase with the rf voltage $\tilde{V}_{\rm rf}$. First, we have $i_0 = V_{\rm rf}/R_L$, so that Robinson's criterion of phase stability in Eq. (8.47) can be rewritten as

$$\frac{i_{\rm im}}{i_0} < \frac{\cos\phi_s}{\sin\psi\cos\psi} \qquad \begin{cases} \psi > 0 & \text{below transition,} \\ \psi < 0 & \text{above transition.} \end{cases} \tag{8.50}$$

Second, the in-phase condition implies Eq. (8.30), which simplifies the above to

$$\frac{i_{\rm im}}{i_0} < \frac{1}{\sin\phi_s} \ , \tag{8.51}$$

after eliminating the detuning. If we further optimize the generator power by choosing the coupling constant $\beta_{\rm op}$ given by Eq. (8.39), it is easy to show that

$$\frac{i_{im}\sin\phi_s}{i_0} = \frac{\beta_{\rm op}-1}{\beta_{\rm op}+1} < 1 \ . \tag{8.52}$$

In other words, the Robinson's phase stability criterion will always be satisfied when the generator current phasor $\tilde{i}_g$ and the rf voltage phasor $\tilde{V}_{\rm rf}$ are in phase and the coupling between the generator and the rf cavities is optimized.

When the generator current phasor and the rf voltage phasor are in phase, Fig. 8.6 immediately gives the phase stability limiting criterion for the detuning as

$$\psi = \frac{\pi}{2} - \phi_s \ . \tag{8.53}$$

Substituting into the in-phase condition of Eq. (8.30) reproduces the stability criterion of Eq. (8.51). The stability criterion can also be rewritten as

$$\tfrac{1}{2}V_{\rm rf}i_{\rm im}\sin\phi_s < \tfrac{1}{2}V_{\rm rf}i_0 \ , \tag{8.54}$$

where the right side is P_L, the power dissipated in the cavities and the generator, while the left side is P_b, the power supplied to the beam for acceleration and/or compensation of energy lost to radiation and impedance. Thus, Robinson's phase stability criterion can also be reworded as

$$P_b < P_L \ , \tag{8.55}$$

or the power allocated to dissipation is larger than the power delivered to the beam.

The Robinson's limit of phase stability is correct only if there is no other stabilizing mechanism available. In an accelerator ring, there is usually a loop that monitors the beam loading and feedbacks onto the generator current so as to maintain the required rf gap voltage and synchronous phase. This correction, however, is not instantaneous, because it takes time for the new generator voltage to establish inside the rf cavity. If gain of the feedback is high, the time delay can be much faster than the fill time $T_f = 2Q_L/\omega_r$ of the cavity. If this time delay is short compared with the synchrotron period, phase stability can be established, even if the criterion $P_b < P_L$ is violated. The former Fermilab Main Ring at its peak intensity of $N_p = 3.25 \times 10^{13}$ protons/pulse (about 3.25×10^{10} per bunch for 1000 bunches) serves as an example. The ring had a mean radius of 1 km and therefore a revolution frequency $f_0 = 47.7$ kHz. The dc beam current was $I_0 = eN_pf_0 = 0.245$ A or the image current was $i_{\rm im} = 2I_0 = 0.490$ A assuming that the bunches are short. With 15 working cavities each supplying 213 kV, the total rf voltage was $V_{\rm rf} = 3.2$ MV. The acceleration rate was 125 GeV/s or 2.62 MeV/turn. Thus, $\sin\phi_s = 0.819$ and $i_{\rm im}\sin\phi_0 = 0.407$ A. Each cavity had a loaded shunt impedance of 0.60 MΩ, or the total loaded shunt impedance was $R_L = 9.00$ MΩ. The current required to set up the rf voltage turned out to be $i_0 = V_{\rm rf}/R_L = 0.355$ A, which less than $i_{\rm im}\sin\phi_0$. Thus, Robinson's phase stability criterion had been violated. There was a servo-tuner that guaranteed the generator current phasor to be in-phase with with rf voltage phasor. There were also rf voltage magnitude and phase loops to maintain the the proper rf voltage and synchronous phase. The rf cavities were of $\omega_r/(2\pi) = 53.1$ MHz with a loaded quality factor $Q_L \approx 5000$. The cavity fill time was then $T_f = 30.0$ μs or about 1.43 revolution turns, small compared with the synchrotron period of ~ 100 turns. The modification of the detuning is usually the slowest part of the feedback procedure, but it is definitely faster than the synchrotron frequency. As a result, phase stability was maintained even when Robinson's stability criterion was not fulfilled.

8.3.3   Robinson's Damping

Next, we consider the interaction of the beam with the impedance of the rf system. As we will see, proper detuning damps synchrotron oscillations while improper detuning leads to an oscillation with increasing amplitude. During half of a synchrotron period, the center of the bunch is at a higher energy than the synchronous particle. For the sake of convenience, choose the particular moment when the phase of bunch center is just in phase with the synchronous particle, so that the phasor $\tilde{i}_b$ is exactly along the x-axis.
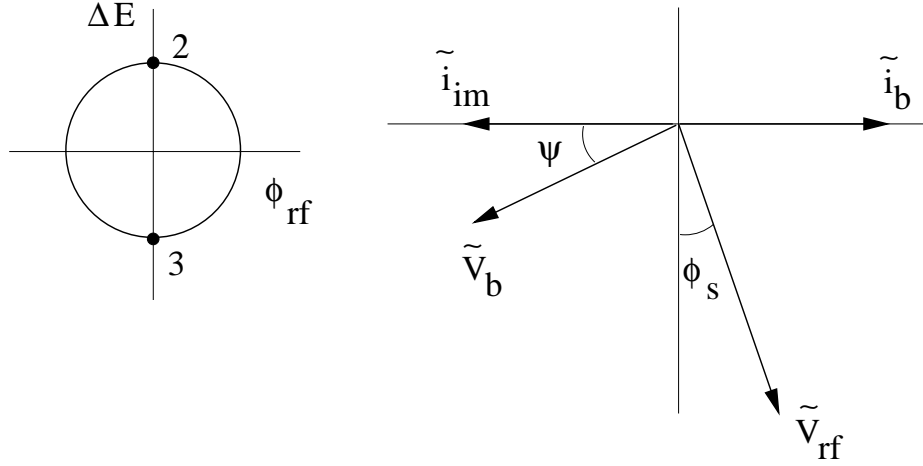
Figure 8.7: With bunch center at Point 2 in the synchrotron oscillation, the beam current phasor $\tilde{i}_b$ is in phase with the x-axis in the phasor plot. Below transition, higher energy implies higher effective rf frequency ω_{rf}. The bunch sees a smaller effective detuning angle and loses more energy per turn than when the bunch is at the synchronous position. The synchrotron oscillation amplitude is therefore damped.

This is illustrated by Point 2 in the synchrotron oscillation and the beam current phasor being in phase with the x-axis in the phasor plot in Fig. 8.7. Below transition, however, higher energy implies higher revolution frequency ω_0. The detuning ψ which is defined by

$$\tan\psi = 2Q_L \frac{\omega_r - \omega_{\mathrm{rf}}}{\omega_r} \tag{8.56}$$

appears effectively smaller from the view of the bunch center, when we consider the effective rf frequency as $\omega_{\mathrm{rf}} = h\omega_0$. The energy loss per turn, which is $i_{im}|Z_{\mathrm{cav}}|\cos\psi$, will be larger than if the bunch center is synchronous. For the other half of the synchrotron period, the beam particle has an energy smaller than the synchronous particle and revolves with a lower frequency, and therefore sees a larger effective detuning. Again we choose the moment when the phase of the bunch center is just in phase with synchronous particle, or Point 3 in the synchrotron oscillation. The bunch will lose less energy than if it is synchronous. The result is a gradual decrease in the energy offset oscillation after oscillation. This reduction of synchrotron oscillation amplitude is called *Robinson damping*. Notice that if the detuning is in the other direction below transition, $\psi < 0$, the beam particle will lose less energy when its energy is higher than synchronous and lose more energy when its energy is less. The oscillation amplitude will increase turn

after turn and the beam will therefore be Robinson unstable. The opposite is true if the beam is above transition. We therefore have the criterion of Robinson stability:

$$\begin{cases} \psi > 0 \quad \text{or} \quad \omega_r > \omega_{\text{rf}} \qquad \text{below transition,} \\ \psi < 0 \quad \text{or} \quad \omega_r < \omega_{\text{rf}} \qquad \text{above transition.} \end{cases} \tag{8.57}$$

Notice that so far we have not imposed any optimization condition on the rf system. If the cavity tuning is adjusted so that the generator current $\tilde{i}_g$ is in the same direction as the rf voltage $\tilde{V}_{\text{rf}}$, so that the beam-cavity impedance appears to be real as demonstrated in Fig. 8.4, the beam will always be Robinson stable, because the detuning will always satisfy Eq. (8.57) according to Eq. (8.30).

8.4   Transient Beam Loading

By transient we mean that the fill time of the cavity T_f is not necessarily much longer than the time interval T_b for successive bunches to pass through the cavity. In other words, the beam loading voltage from the first bunch will have significant decay before the successive bunch arrives.

First, let us understand how the transient beam loading occurs. As the bunch of charge $q > 0$ passes through the cavity gap, a negative charge equal to that carried by the bunch will be left by the image current at the upstream end of the cavity gap. Since the negative image current will resume from the downstream end of the cavity gap following the bunch, an equal amount of positive charge will accumulate there. Thus, a voltage will be created at the gap opposing the beam current and this is the transient beam loading voltage as illustrated in Fig. 8.8. For an infinitesimally short bunch, this transient voltage is

$$V_{b0} = \frac{q}{C} = \frac{q\omega_r R_s}{Q_0} \ , \tag{8.58}$$

where C is the equivalent capacitance across the gap of the cavity. Notice that we will arrive at the same value if the loaded shunt impedance R_L and the loaded quality factor Q_L are used instead. Due to the finite quality factor Q_0, this induced voltage across the gap starts to decay immediately, hence the name transient beam loading. We will give concrete example about the size of the voltage later. The next question is how much of this beam loading voltage will be seen by the bunch. This question is answered by the fundamental theorem of beam loading first derived by P. Wilson [1].
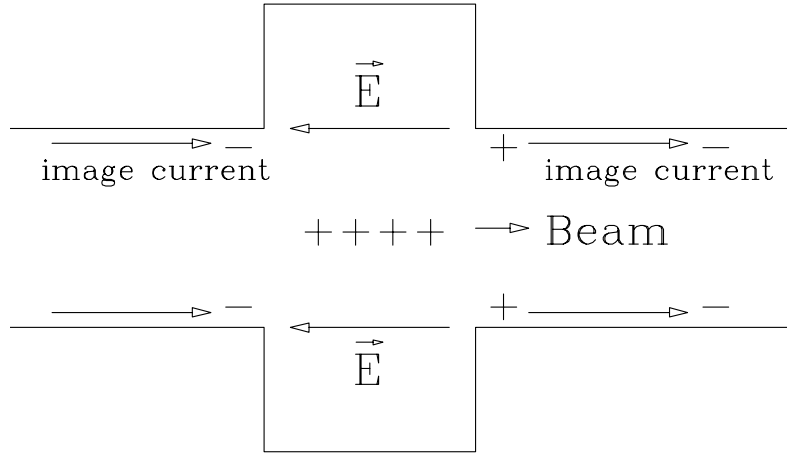
Figure 8.8: As a positively charged bunch passes through a cavity, the image current leaves a negative charge at the upstream end of the cavity gap. As the image current resumes at the downstream side of the cavity, a positive charge is created at the downstream end of the gap because of charge conservation, thus setting up an electric field $\vec{E}$ and therefore the induced beam loading voltage.

8.4.1   Fundamental Theorem of Beam Loading

When a particle of charge q passes through a cavity that is lossless (infinite R_s and infinite Q_0), it induces a voltage V_{b0} which will start to oscillate with the resonant frequency of the cavity. Suppose that the particle sees a fraction f of V_{b0}, which opposes its motion. After half an oscillation of the cavity, a second particle of charge q passes through the cavity. The first induced voltage left by the first is now in the direction of the motion of the second particle and accelerates the particle. At the same time, this second particle will induce another retarding voltage $\tilde{V}_{b0}$ which it will see as a fraction f. This second retarding voltage will cancel exactly the first one inside the cavity, since the cavity is assumed to be lossless. In other words, no field will be left inside the cavity after the passage of the two particles. The net energy gained by the second particle is

$$\Delta E_2 = qV_{b0} - fqV_{b0} \; , \tag{8.59}$$

while the first particle gains

$$\Delta E_1 = -fqV_{b0} \; . \tag{8.60}$$

Conservation of energy requires that the total energy gained by the two particles must be zero. This implies $f = \frac{1}{2}$. In other words, the particle sees one half of its transient beam loading voltage, which is the fundamental theorem of beam loading.
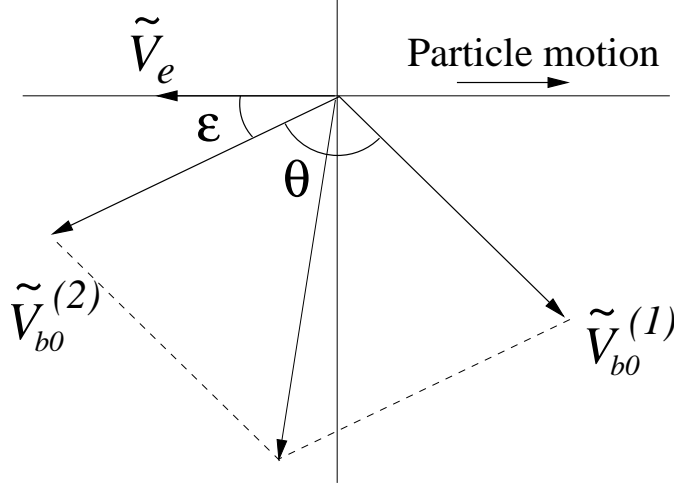
Figure 8.9: Phasor plot showing the the instant just after the second passage of the charged particle through the lossless cavity. The induced beam loading voltage phasors for the two passages are labeled as $V_{b0}^{(1)}$ and $V_{b0}^{(2)}$, respectively.

The following is a more general proof by Wilson. The first particle induces a voltage phasor $\tilde{V}_{b0}^{(1)}$ in the lossless cavity which may lie at an angle ϵ with respect to the voltage $\tilde{V}_e$ seen by that particle. As before, we suppose $V_e = fV_{b0}$, where V_e and V_{b0} are the magnitudes of, respectively, $\tilde{V}_e$ and $\tilde{V}_{b0}^{(1)}$. Some time later when the cavity phase changes by θ, the same particle returns via bending magnets or whatever and passes through the cavity again. It induces a second beam loading voltage phasor $\tilde{V}_{b0}^{(2)}$. At this moment, the phasor $\tilde{V}_{b0}^{(1)}$ rotates to a new position as illustrated in Fig. 8.9. The net energy lost by the particle on the two passes is

$$\Delta E = 2fqV_{b0}\cos\epsilon + qV_{b0}\cos(\epsilon + \theta) \ . \tag{8.61}$$

The cavity, however, gains energy because of the beam loading fields left behind. The energy inside a cavity is proportional to the square of the gap voltage. If the cavity is free of any field to start with, the final energy stored there becomes

$$\Delta E_c = \alpha \left(2V_{b0}\cos\frac{\theta}{2} \right)^2 = 2\alpha V_{b0}^2 (1 + \cos\theta) \ , \tag{8.62}$$

where α is a proportionality constant. From the conservation of energy, we get

$$2fqV_{b0}\cos\epsilon + qV_{b0}(\cos\epsilon\cos\theta - \sin\epsilon\sin\theta) - 2\alpha V_{b0}^2(1 + \cos\theta) = 0 \ . \tag{8.63}$$

Since θ is an arbitrary angle, we obtain

$$qV_{b0}\sin\epsilon = 0 \ ,$$

$$qV_{b0}\cos\epsilon = 2\alpha V_{b0}^2 \ ,$$

$$2fqV_{b0}\cos\epsilon = 2\alpha V_{b0}^2 \ . \tag{8.64}$$

The first equation gives $\epsilon = 0$ implying that the transient beam loading voltage must have a phase such as to maximally oppose the motion of the inducing charge. Clearly $\epsilon = \pi$ will not be allowed because this leads to the unphysical situation of the particle gaining energy from nowhere. Solving the other two equations, we obtain $f = \frac{1}{2}$.

8.4.2   From Transient to Steady State

Let the bunch spacing be h_b rf buckets or T_b in time. The cavity time constant or filling time is $T_f = 2Q_L/\omega_r$ and the e-folding voltage decay decrement between two successive bunch passages is $\delta_L = T_b/T_f$. During this time period, the phase of the rf fields changes by $\omega_r T_b$ and the rf phase by $\omega_{\rm rf}T_b = 2\pi h_b$. The phasors therefore rotate by the angle $\Psi = \omega_r T_b - 2\pi h_b$, which can also be written in terms of the detuning angle,

$$\Psi = (\omega_r - \omega_{\rm rf})T_b = \delta_L \tan\psi \ , \tag{8.65}$$

where Eq. (8.24) has been used. The transient beam loading voltage left by the first passage of a short bunch carrying charge q is $V_{b0} = q/C = q\omega_r R_L/Q_L$. The total beam loading voltage V_b seen by a short bunch is obtained by adding up vectorially the beam loading voltage phasors for all previous bunch passages. The result is

$$V_b = \tfrac{1}{2}V_{b0} + V_{b0}\left(e^{-\delta_L}e^{j\Psi} + e^{-2\delta_L}e^{j2\Psi} + \cdots\right) \ , \tag{8.66}$$

where the $\frac{1}{2}$ in the first term on the right side is the result of Wilson's fundamental theorem of beam loading, which states that a particle sees only one-half of its own induced voltage. It is worth pointing out that these voltages are excitations of the cavity and are therefore oscillating at the cavity resonant frequency (all higher order modes of the cavity are neglected). This infinite series of induced voltage phasors is illustrated in Fig. (8.10). The summation can be performed exactly giving the result

$$V_b = V_{b0}\Big[F_1(\delta_L,\psi) + jF_2(\delta_L,\psi)\Big] \ , \tag{8.67}$$

with

$$F_1 = \frac{1 - e^{-2\delta_L}}{2D} \ , \qquad F_2 = \frac{e^{-\delta_L}\sin(\delta_L\tan\psi)}{D} \ , \tag{8.68}$$
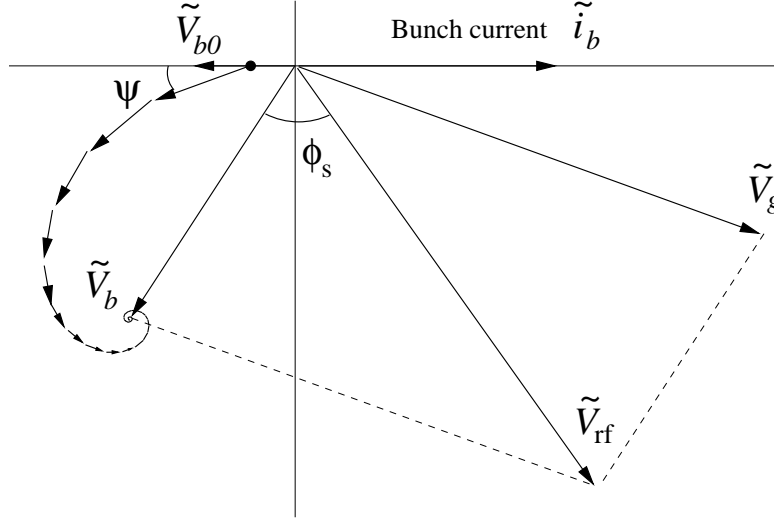
Figure 8.10: Transient beam loading voltages from equally spaced bunches. Each preceding voltage phasor has a phase advance of ψ because of detuning and a decay of $e^{-\delta_L}$. Note that the bunch that is just passing by sees only half of its induced voltage $\tilde{V}_{b0}$. These voltage phasors add up to the total beam loading voltage phasor $\tilde{V}_b$. Together with the generator voltage $\tilde{V}_g$, the cavity gap voltage results at the synchronous angle ϕ_s.

$$D = 1 - 2e^{-\delta_L}\cos(\delta_L \tan\psi) + e^{-2\delta_L} \ . \tag{8.69}$$

In terms of the coupling constant β and detuning angle ψ, we have

$$\begin{aligned}
\tan\psi &= 2Q_L \frac{\omega_r - \omega_{\text{rf}}}{\omega_r} \ , \\
Q_L &= \frac{Q_0}{1+\beta} \ , \\
\delta_L &= \delta_0(1+\beta) \ ,
\end{aligned} \tag{8.70}$$

where we have defined $\delta_0 = T_b/T_{f0}$ with T_{f0} being the filling time of the unloaded cavity. Then the single bunch induced beam loading voltage becomes

$$V_{b0} = 2I_0 R_s \delta_0 \ , \tag{8.71}$$

use has been made of the approximation for short bunches, so that the Fourier component of the current of a bunch at frequency ω_{rf}/h_b is equal to twice its dc value or $i_b = 2I_0$ and $I_0 = q/T_b$. Putting things together, we get

$$V_b = 2I_0 R_s \delta_0 \left[F_1(\delta_0, \beta, \psi) + jF_2(\delta_0, \beta, \psi) \right] \ , \tag{8.72}$$

with

$$F_1(\delta_0, \beta, \psi) = \frac{1 - e^{-\delta_0(1+\beta)}}{2D} \ , \tag{8.73}$$

$$F_2(\delta_0, \beta, \psi) = \frac{e^{-\delta_0(1+\beta)} \sin[\delta_0(1+\beta)\tan\psi]}{D} \ , \tag{8.74}$$

$$D = 1 - 2e^{-\delta_0(1+\beta)} \cos[\delta_0(1+\beta)\tan\psi] + e^{-2\delta_0(1+\beta)} \ . \tag{8.75}$$

Some comments are in order. Figure 8.10 shows the transient nature of beam loading if the beam loading voltage phasors, that rotate by the angle Ψ and have their magnitudes diminished by the factor $e^{-\delta_L}$ for each successive time period, are excitations of *one* short bunch. However, what we consider is in fact the diminishing beam loading voltage phasors coming from successive bunches that pass through the cavity at successive time periods nT_b earlier with $n = 1, 2, \cdots$. For this reason, what Fig. 8.10 shows is actually the steady-state situation of the beam loading voltages, because for each time interval T_b later, we will see exactly the same spiraling beam loading phasor plot and the same total beam loading voltage phasor $\tilde{V}_b$. Therefore, we can add into the plot the generator voltage phasor $\tilde{V}_g$ in the same way as the plot in Fig. 8.4. In fact, the plot in Fig. 8.4 provides only an approximate steady-state plot, because the beam loading voltage phasor there does attenuate a little bit after a 2π rotation of the phasors, although a high Q_L has been assumed. However, such attenuation has already been taken care of in Fig. 8.10, resulting in the plotting of an exact steady state. When the bunch arrives, the beam loading voltage phasor is $\tilde{V}_b$ as indicated in Fig. 8.10. It rotates counterclockwise and its magnitude decreases because of finite quality factor of the cavity. Just before the arrival of the next bunch, the beam loading voltage phasor becomes $\tilde{V}_b - \frac{1}{2}\tilde{V}_{b0}$. Notice that the beam loading voltage phasor rotates for more than 2π, since $\omega_r > \omega_{\rm rf}$ or the detuning angle ψ is positive in Fig. 8.10. As soon as the next bunch arrives, it jumps by $\frac{1}{2}\tilde{V}_{b0}$ and goes back to $\tilde{V}_b$. Therefore, the beam loading voltage phasor is not sinusoidal and does not rotate at the speed of $\omega_{\rm rf}$ or $\omega_{\rm rf}/h_b$. It approaches sinusoidal only when the jump of the transient beam loading voltage $\frac{1}{2}\tilde{V}_{b0}$ is small and that happens when the loaded quality factor Q_L is large, or when the cavity filling time $T_f = 2Q_L/\omega_r$ is much larger than the time interval T_b between successive bunch passages. On the other hand, the beam loading voltage phasor $\tilde{V}_b$ seen by the bunch in Fig. 8.4 is sinusoidal because it is induced by a sinusoidal component of the beam. In fact, over there, we allow for only one Fourier component.

Using Eq. (8.14), the generator power P_g can now be computed:

$$P_g = \frac{(1+\beta)^2 V_{\rm rf}^2}{8\beta R_s \cos^2 \psi} \left\{ \left[\sin\phi_s - \frac{i_b R_s \delta_0}{V_{\rm rf}} F_1(\delta_0, \beta, \psi) \right]^2 + \left[\cos\phi_s + \frac{i_b R_s \delta_0}{V_{\rm rf}} F_2(\delta_0, \beta, \psi) \right]^2 \right\} .$$
$$(8.76)$$

In the situation when the generator current $\tilde{i}_g$ is in phase with the rf voltage $\tilde{V}_{\rm rf}$, the generator power can be minimized so that there will not be any reflection. Similarly, the generator power can also be optimized by choosing a suitable coupling coefficient β. Unfortunately, these optimized powers cannot be written as simple analytic expressions.

8.4.2.1   Limiting Case with $\delta_0 \to 0$

When the bunch spacing T_b is short compared to the unloaded cavity filling time T_{f0}, simplified expressions can be written for the total beam loading voltage V_b. One gets

$$F_1(\delta_0, \beta, \psi) = \frac{1}{\delta_0 (1+\beta)(1+\tan^2\psi)} , \qquad (8.77)$$

$$F_2(\delta_0, \beta, \psi) = \frac{\tan\psi}{\delta_0 (1+\beta)(1+\tan^2\psi)} , \qquad (8.78)$$

so that

$$V_b = \frac{i_b R_s}{1+\beta} \frac{1}{1 - j\tan\psi} . \qquad (8.79)$$

Notice that this is exactly the same expression in Eq. (8.25). In fact, this is to be expected, because we are in the situation of $T_b \ll T_f$, or the case of a high Q_L resonating cavity.

In the absence of detuning, the beam loading voltages left by previous bunches just added up to give

$$V_b = \frac{V_{b0}}{2} \frac{1 + e^{-\delta_L}}{1 - e^{-\delta_L}} . \qquad (8.80)$$

For a high-Q_L cavity, this becomes

$$V_b = \frac{V_{b0}}{\delta_L} = i_b R_L , \qquad (8.81)$$

which is the maximum beam loading voltage seen by the beam.

When $\delta_0 \to 0$, the phase angle $\Psi = \delta_0(1+\beta)\tan\psi \to 0$, although the detuning ψ may be finite. Thus, the transient beam loading voltage $\tilde{V}_{b0}$ will not decay and will

also line up for successive former bunch passages, leading to an infinite total beam loading voltage V_b seen by the bunch. However, $\delta_0 \to 0$ implies letting $Q_0 \to \infty$ while keeping the shunt impedance fixed. Thus, the instantaneous beam loading voltage $V_{b0} = q/C = q\omega_r R_s/Q_0 = 2i_b R_s \delta_0$ also goes to zero, implying that the summation has to be done with care. For successive V_{b0}'s to wrap around in a circle, one needs approximately $2\pi/\Psi$ V_{b0}'s. The radius of this circle will be V_{b0}/Ψ. As $\delta_0 \to 0$, this radius becomes

$$\lim_{\delta_0 \to 0} \frac{V_{b0}}{\Psi} = \frac{2i_b R_s}{\tan\psi} \; , \tag{8.82}$$

which is finite. In fact, this is roughly the same as the total beam loading voltage V_b as $\delta_0 \to 0$.

During bunch-to-bunch injection, the transient beam loading voltage in the cavity will add up gradually as is indicated in the spiral in Fig. 8.10. Thus, if the decay decrement is small, the total beam loading voltage will reach a maximum roughly equal to twice the voltage given by Eq. (8.72) before spiraling to its limiting value. The maximum beam loading voltage will be twice the value given by Eq. (8.79) as if the shunt impedance has been doubled.

8.4.2.2   Limiting Case with $T_b \gg T_f$

This is the situation when the instantaneous beam loading voltage decays to zero before a second bunch comes by. It is easy to see that $F_1(\delta_0, \beta, \psi) \to \frac{1}{2}$ and $F_2(\delta_0, \beta, \psi) \to 0$. From Eq. (8.76), it is clear that the generator power increases rapidly as the square of δ_0. This is easy to understand, because the rf power that is supplied to the cavity gets dissipated rapidly. A pulse rf system will then be desirable. In such a system, the power is applied to the cavity for about a filling time preceding the arrival of the bunch. For most of the time interval between bunches, there is no stored energy in the cavity at all and hence no power dissipation.

8.4.3   Transient Beam Loading of a Bunch

When a bunch of linear density $\rho(\tau)$ passes through a cavity gap, electromagnetic fields are excited. The beam loading retarding voltage seen by a particle at time τ ahead of

the bunch center is given by

$$V(\tau) = \int_\tau^\infty q\rho(\tau')W_0'(\tau' - \tau)d\tau' , \qquad (8.83)$$

where q is the total charge in the bunch, $\rho(\tau)$ is normalized to unity when integrated over τ, and $W_0'(\tau)$ is the wake potential left by a point charge at a time τ ago. If we approximate the cavity as a RLC parallel circuit with angular resonant frequency ω_r, loaded quality factor Q_L, and loaded shunt impedance R_L, the wake potential can be written as, for $\tau > 0$,

$$W_0'(\tau) = \frac{\omega_r R_L}{Q_L}e^{-\alpha\tau}\left[\cos\bar\omega\tau - \frac{\alpha}{\bar\omega}\sin\bar\omega\tau\right] . \qquad (8.84)$$

For $\tau < 0$, $W_0'(\tau) = 0$ because of causality. For $\tau = 0$, $W_0'(\tau) = \omega_r R_L/(2Q_L)$ because of the fundamental theorem of beam loading. In above, the decay rate α and the shifted resonant angular frequency $\bar\omega$ are given by

$$\alpha = \frac{\omega_r}{2Q_L} \qquad \text{and} \qquad \bar\omega = \sqrt{\omega_r^2 - \alpha^2} . \qquad (8.85)$$

Notice that this is exactly the same wake potential we studied in Eq. (1.48) of Exercise 1.3. For the convenience of derivation, we introduce the loss angle θ which is defined as[‡]

$$\cos\theta = \frac{\bar\omega}{\omega_r} \qquad \text{and} \qquad \sin\theta = \frac{\alpha}{\omega_r} . \qquad (8.86)$$

With this introduction, the wake potential can be conveniently rewritten as

$$W_0'(\tau) = \frac{\omega_r R_L}{Q_L\cos\theta}\mathcal{R}e\, e^{i(e^{i\theta}\omega_r\tau+\theta)} . \qquad (8.87)$$

The first application is for a point bunch with distribution $\rho(\tau) = \delta(\tau)$. Substitution into Eq. (8.83) gives $V(\tau) = qW_0'(-\tau)$, or

$$V(\tau) = \begin{cases} 0 & \tau > 0 , \\[2ex] \dfrac{q\omega_r R_L}{2Q_L} & \tau = 0 , \\[2ex] \dfrac{q\omega_r R_L}{Q_L\cos\theta}\mathcal{R}e\, e^{i(e^{i\theta}\omega_r\tau+\theta)} & \tau < 0 . \end{cases} \qquad (8.88)$$

Thus, the head of the bunch ($\tau = 0+$) sees no beam loading voltage. The tail of the bunch ($\tau = 0-$) sees the transient beam loading voltage $V_{b0} = q/C$ as given by Eq. (8.58). The center of the bunch sees one half of V_{b0}.

[‡]If one prefers, this angle can also be defined as $\cos\theta = \alpha/\omega_r$ and $\sin\theta = \bar\omega/\omega_r$.

8.4.3.1   Gaussian Distribution

Consider a Gaussian distributed bunch of rms length σ_τ. The linear density is

$$\rho(\tau) = \frac{1}{\sqrt{2\pi}\sigma_\tau} e^{-\tau^2/(2\sigma_\tau^2)} \ . \tag{8.89}$$

The beam loading voltage experienced by a beam particle at distance τ ahead the bunch center is (Exercise 8.5)

$$V(\tau) = \frac{q\omega_r R_L}{2Q_L \cos\theta} \, \mathcal{R}e \, e^{i\theta - \tau^2/(2\sigma_\tau^2)} \, w\left(\frac{\sigma_\tau \omega_r e^{i\theta}}{\sqrt{2}} + \frac{i\tau}{\sqrt{2}\sigma_\tau}\right) \ , \tag{8.90}$$

where q is the total charge in the bunch and w is the complex error function defined as

$$w(z) = e^{-z^2}\left[1 + \frac{2i}{\sqrt{\pi}}\int_0^z e^{t^2}dt\right] \ . \tag{8.91}$$

It can be readily shown that as the bunch length shortens to zero, the head, center, and tail of the bunch are seeing the transient beam loading voltage (Exercise 8.5)

$$V(\tau) = \begin{cases} 0 & \tau = 0+ \ \text{(head)} \ , \\[2mm] \dfrac{q\omega_r R_L}{2Q_L} & \tau = 0 \quad \text{(center)} \ , \\[2mm] \dfrac{q\omega_r R_L}{Q_L} & \tau = 0- \ \text{(tail)} \ , \end{cases} \tag{8.92}$$

exactly the same result for a point bunch. In fact, Eq. (8.92) just serves as another proof of the fundamental theorem of beam loading that the test charge sees one half of its own beam loading voltage. This proof is more general than those presented in the previous subsection, because it involves a lossy cavity or a cavity with a finite quality factor Q_L.

The beam loading voltages of a Gaussian bunch are plotted in Fig. 8.11. They are all normalized to $q\omega_r R_L/Q_L$, which is the beam loading voltage when the bunch is contracted to a point. Each curve is identified by two parameters: (Q_L, F), where $F = \sqrt{6}\omega_r\sigma_\tau/\pi$ is roughly the fraction of the rf wavelength occupied by the bunch, since we usually equate the half 95% Gaussian bunch length to $\sqrt{6}\sigma_\tau$. The horizontal coordinate is the distance of the test particle ahead the bunch center in units of σ_τ, the rms bunch length. We notice that as the bunch becomes shorter, the beam loading voltage becomes larger. When it becomes very short, the curve with (1,0.01), we recover the
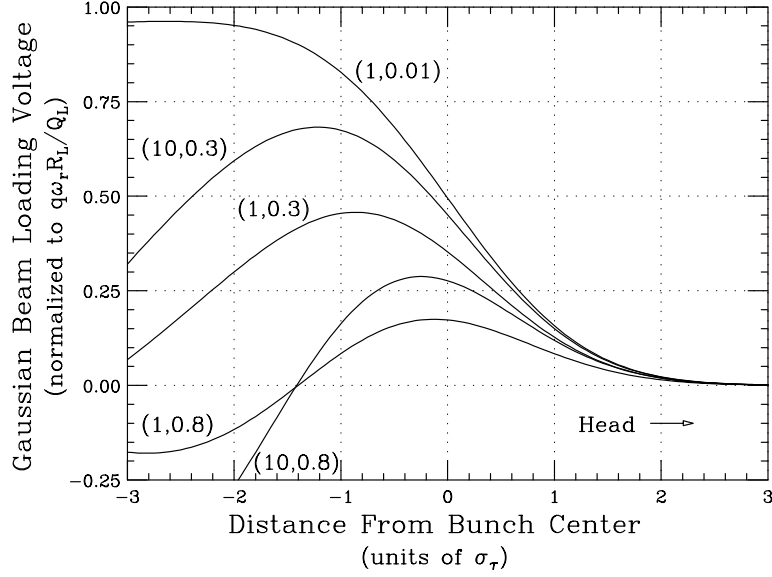
Figure 8.11: The beam loading voltage, normalized to $q\omega_r R_L/Q_L$, of a bunch with Gaussian distribution seen by a particle at distance τ/σ_τ ahead the bunch center, where σ_τ is the bunch rms length and q the total charge in the bunch. Each curve is labeled by (Q_L, F), where $F = \sqrt{6}\omega_r\sigma_\tau/\pi$ is roughly the fraction of the rf wavelength occupied by the bunch, and Q_L, R_L, and $\omega_r/(2\pi)$ are, respectively, the loaded quality factor, loaded shunt impedance, and resonant frequency of the cavity.

results in Eq. (8.92) that a particle at the center of the bunch sees one half of the bunch beam loading voltage. When the quality factor of the cavity becomes larger, the beam loading voltage does not decay as fast and its reduced amplitude is therefore closer to unity. We also notice that the beam loading voltage seen by each particle in the bunch varies along the bunch. This result is important, because it is difficult to compensate for the beam loading voltage to every point along the bunch.

8.4.3.2   Parabolic Distribution

Consider a bunch with parabolic distribution,

$$\rho(\tau) = \frac{3}{4\hat{\tau}}\left(1 - \frac{\tau^2}{\hat{\tau}^2}\right) \qquad |\tau| \le \hat{\tau} \; , \tag{8.93}$$

where $\hat{\tau}$ is the half bunch length. As the bunch of total charge q passes through a cavity, the transient beam loading voltage seen by a particle at a distance T behind the head

of the bunch is (Exercise 8.6), for $T \leq 2\hat{\tau}$,

$$
V(T) = \frac{q\omega_r R_L}{Q_L} \frac{3p^2}{2\pi^2 \cos\theta} \left\{ \frac{p}{\pi} \left[\omega_r(\hat{\tau}-T)\cos\theta + \sin 2\theta\right] + \right.
$$
$$
\left. + e^{-\alpha T}\left[\sin(\bar{\omega}T - 2\theta) - \frac{p}{\pi}\cos(\bar{\omega}T - \theta)\right]\right\} , \qquad (8.94)
$$

and for $T > 2\hat{\tau}$,

$$
V(T) = \frac{q\omega_r R_L}{Q_L} \frac{3p^2}{2\pi^2 \cos\theta} \left\{ e^{-\alpha(T-2\hat{\tau})}\left[\frac{p}{\pi}\sin\left(\bar{\omega}(T-2\hat{\tau}) - 2\theta\right) - \cos\left(\bar{\omega}(T-2\hat{\tau}) - \theta\right)\right] + \right.
$$
$$
\left. + e^{-\alpha T}\left[\sin(\bar{\omega}T - 2\theta) - \frac{p}{\pi}\cos(\bar{\omega}T - \theta)\right]\right\} , \qquad (8.95)
$$

where

$$
p = \frac{\pi}{\omega_r \hat{\tau}} . \qquad (8.96)
$$

Beside the normalization factor $q\omega_r R_L/Q_L$, the beam loading voltage depends on two parameters: $\omega_r \hat{\tau}$ and the loaded quality factor Q_L.

Figure 8.12 shows the beam loading voltage seen by a bunch with parabolic distribution. The normalization is also to $q\omega_r R_L/Q_L$. The horizontal coordinate is the fractional distance $T/(2\hat{\tau})$ of the test particle behind the head of the bunch. Each voltage curve is labeled by the two parameters (Q_L, F), where $F = \omega_r \hat{\tau}/\pi = 1/p$ is the ratio of the total bunch length to the rf wavelength. All the comments of the beam loading voltage of the Gaussian bunch apply here also.

8.4.3.3   Cosine-Square Distribution

Consider a bunch with cosine-square linear distribution,

$$
\rho(\tau) = \frac{1}{\hat{\tau}}\cos^2 \frac{\pi\tau}{2\hat{\tau}} \qquad |\tau| \leq \hat{\tau} , \qquad (8.97)
$$

where $\hat{\tau}$ is the half bunch length. As the bunch of total charge q passes through a cavity, the transient beam loading voltage seen by a particle at a distance T behind the head
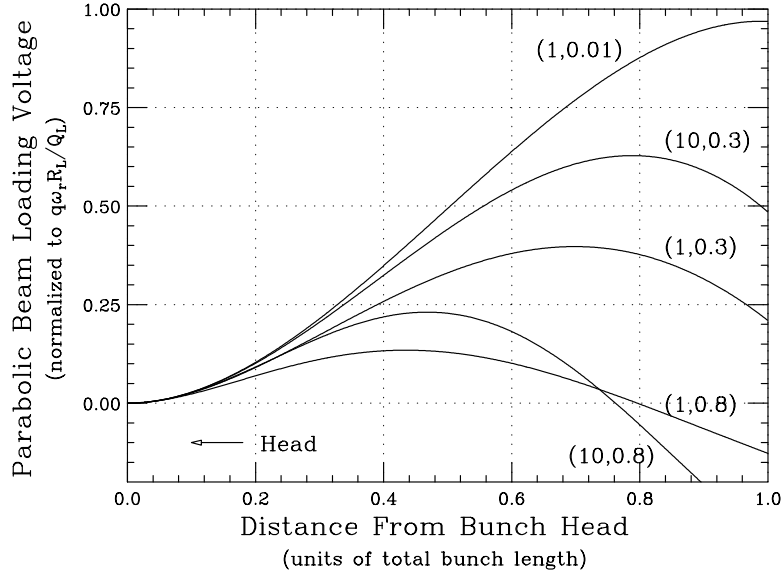
Figure 8.12: The beam loading voltage, normalized to $q\omega_r R_L/Q_L$, of a bunch with parabolic distribution seen by a particle at distance $T/(2\hat{\tau})$ behind of the head of the bunch, where $2\hat{\tau}$ is the total bunch length and q the total charge in the bunch. Each curve is labeled by (Q_L, F), where $F = \omega_r \hat{\tau}/\pi$ is the fraction of the rf wavelength occupied by the bunch, and Q_L, R_L, and $\omega_r/(2\pi)$ are, respectively, the loaded quality factor, loaded shunt impedance, and resonant frequency of the cavity.

of the bunch is (Exercise 8.6), for $T \leq 2\hat{\tau}$,

$$V(T) = \frac{q\omega_r R_L}{Q_L} \frac{p^2}{2\pi D \cos\theta} \left\{ \left(1 - p^2\right) \sin\frac{\pi(\hat{\tau}-T)}{\hat{\tau}} \cos\theta + p\cos\frac{\pi(\hat{\tau}-T)}{\hat{\tau}} \sin 2\theta + \right.$$

$$\left. + p^3 e^{-\alpha T} \sin\bar{\omega}T - p e^{-\alpha T}\sin(\bar{\omega}T-2\theta) \right\} , \qquad (8.98)$$

and for $T > 2\hat{\tau}$,

$$V(T) = \frac{q\omega_r R_L}{Q_L} \frac{p^2}{2\pi D \cos\theta} \left\{ p e^{-\alpha(T-2\hat{\tau})} \sin\left[\bar{\omega}(T-2\hat{\tau}) - 2\theta\right] - p^3 e^{-\alpha(T-2\hat{\tau})}\sin\bar{\omega}(T-2\hat{\tau}) + \right.$$

$$\left. + p^3 e^{-\alpha T} \sin\bar{\omega}T - p e^{-\alpha T}\sin\left(\bar{\omega}T-2\theta\right) \right\} , \qquad (8.99)$$

where p is given by Eq. (8.96) and

$$D = 1 - 2p^2 \cos 2\theta + p^4 . \qquad (8.100)$$

Besides the factor outside the curly brackets, the beam loading voltage depends on two parameters: $\omega_r \hat{\tau}$ and the loaded quality factor Q_L.

Figure 8.13 shows the beam loading voltage seen by a bunch with cosine-square distribution. The normalization is also to $q\omega_r R_L/Q_L$. The test particle is at the fractional distance $T/(2\hat{\tau})$ behind the head of the bunch. We labeled each reduced beam loading voltage curve by (Q_L, F), where $F = \omega_r\hat{\tau}/\pi = 1/p$ is the ratio of the total bunch length to the rf wavelength. All the comments concerning the beam loading voltage of the Gaussian bunch apply to here as well.
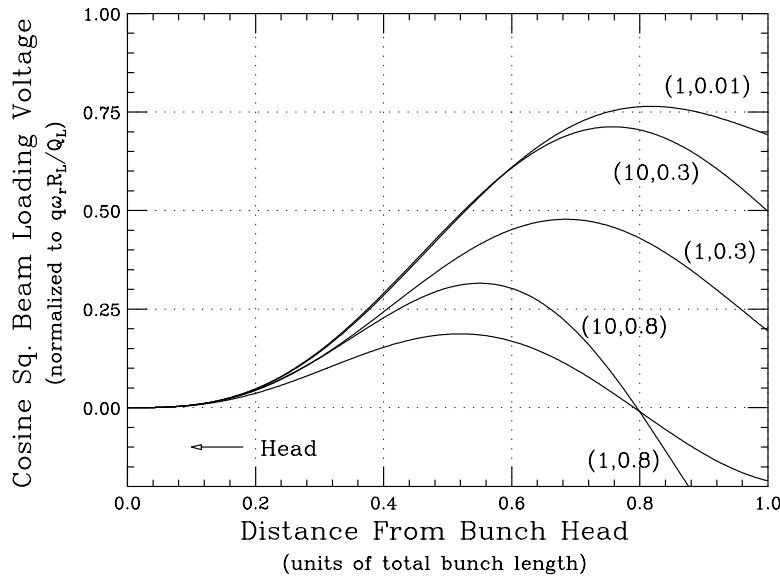

Figure 8.13: The beam loading voltage, normalized to $q\omega_r R_L/Q_L$, of a bunch with cosine-square distribution seen by a particle at distance $T/(2\hat{\tau})$ behind the head of the bunch, where $2\hat{\tau}$ is the total bunch length. Each curve is labeled by (Q_L, F), where $F = \omega_r\hat{\tau}/\pi$ is the fraction of the rf wavelength occupied by the bunch, and Q_L, R_L, and $\omega_r/(2\pi)$ are, respectively, the loaded quality factor, loaded shunt impedance, and resonant frequency of the cavity.

8.4.3.4 Cosine Distribution

Consider a bunch with cosine linear distribution,

$$\rho(\tau) = \frac{\pi}{4\hat{\tau}} \cos\frac{\pi\tau}{2\hat{\tau}} \qquad |\tau| \leq \hat{\tau} , \tag{8.101}$$

where $\hat{\tau}$ is the half bunch length. As the bunch of total charge q passes through a cavity, the transient beam loading voltage seen by a particle at a distance T behind the head

of the bunch is (Exercise 8.6), for $T \leq 2\hat{\tau}$,

$$V(T) = \frac{q\omega_r R_L}{Q_L \cos\theta} \frac{p^2}{8D} \left\{ \left(1 - \frac{p^2}{4}\right) \cos\frac{\pi T}{2\hat{\tau}} \cos\theta + \frac{p}{2} \sin\frac{\pi T}{2\hat{\tau}} \sin 2\theta + \right.$$
$$\left. + e^{-\alpha T}\left[\frac{p^2}{4}\cos(\bar{\omega}T + \theta) - \cos(\bar{\omega}T + \theta)\right] \right\} , \qquad (8.102)$$

and for $T > 2\hat{\tau}$,

$$V(T) = \frac{q\omega_r R_L}{Q_L \cos\theta}\frac{p^2}{8D}\left\{ e^{-\alpha(T-2\hat{\tau})}\left[\frac{p^2}{4}\cos\left(\bar{\omega}(T-2\hat{\tau}) + \theta\right) - \cos\left(\bar{\omega}(T-2\hat{\tau}) - \theta\right)\right] + \right.$$
$$\left. + e^{-\alpha T}\left[\frac{p^2}{4}\cos(\bar{\omega}T+\theta) - \cos(\bar{\omega}T + \theta)\right] \right\} . \qquad (8.103)$$

where p and D are given by Eqs. (8.96) and (8.100). Besides the factor outside the curly brackets, the beam loading voltage depends on two parameters: $\omega_r\hat{\tau}$ and the loaded quality factor Q_L.

Figure 8.14 shows the beam loading voltage seen by a bunch with cosine-square distribution. The normalization is also to $q\omega_r R_L/Q_L$. The test particle is at the fractional distance $T\omega_r/(2\pi)$ behind the head of the bunch, or the time is normalized to an rf wavelength. The reduced beam loading voltage depends on two parameters: $\omega_r\hat{\tau}$ and the loaded quality factor Q_L. We labeled each reduced beam loading voltage curve by (Q_L, F), where $F = \omega_r\hat{\tau}/\pi = 1/p$ is the ratio of the total bunch length to the rf wavelength. All the comments concerning the beam loading voltage of the Gaussian bunch apply to here as well. Both curves are for the high quality factor $Q_L = 5000$. For the example of $F = 0.3$, the reduced transient beam loading voltage has a maximum of 0.681 within the bunch length and later rings for a long time at the frequency $\omega_r/(2\pi)$ of the cavity with an amplitude 0.918 decaying very slowly. This amplitude is roughly equal to $I_1/(2I_0)$, where I_1 is the rf component of the bunch current and I_0 is the average bunch current. Because the e-folding decaying time is Q_L/π rf buckets, the bunch is seeing these ringing amplitudes left by its predecessors. For a ring with all buckets occupied, the beam loading voltage seen by a bunch is

$$V_b = \frac{q\omega_r R_L}{Q_L}\left[A + B\left(1 + e^{-\delta_L} + e^{-2\delta_L} + \cdots\right)\right] , \qquad (8.104)$$

where δ_L is the decay decrement. Here, A denotes the portion of the beam loading voltage excited instantaneously by the bunch crossing the cavity gap while B denotes
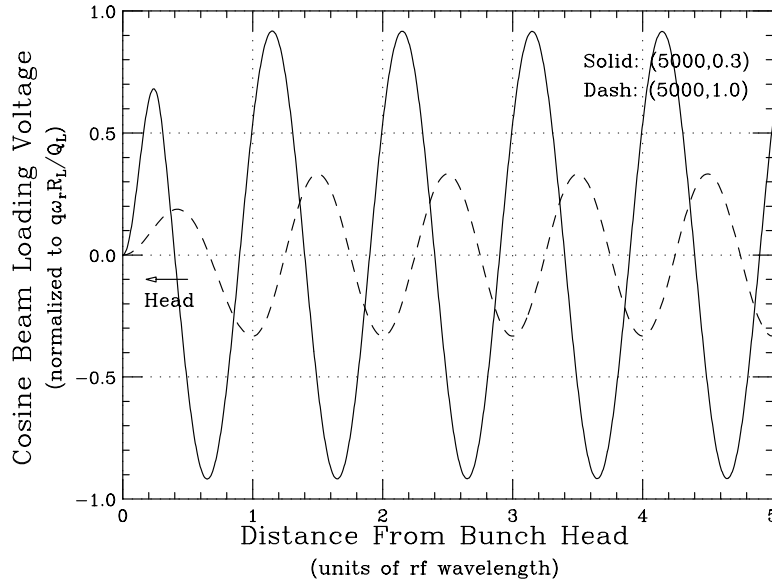
Figure 8.14: The beam loading voltage, normalized to $q\omega_r R_L/Q_L$, of a bunch with cosine distribution seen by a particle at distance T (normalized to the rf wavelength) behind the head of the bunch. Each curve is labeled by (Q_L, F), where $F = \omega_r \hat{\tau}/\pi$ is the fraction of the rf wavelength occupied by the bunch, and Q_L, R_L and $\omega_r/(2\pi)$ are, respectively, the loaded quality factor, loaded shunt impedance, and resonant frequency of the cavity.

whatever left by the previous crossings. Comparing with Eq. (8.66) for a point bunch ($F = 1$), we have $A = \frac{1}{2}$ and $B = 1$. For a bunch of finite extent, for example $F = 0.3$ in the cosine distribution, we have $A = 0.681$ and $B = I_1/(2I_0) = 0.918$. For a high Q_L, it is the second term that dominates. We can conclude that compared with a point bunch, a distributed bunch of finite length will have its beam loading voltage lowered only by a small amount, i.e., by the fraction $I_1/(2I_0)$.

The situation of $F = 1$ is very special and is represented by the dashed curve. Here, the bunch is as long as the rf wavelength. In fact, the situation corresponds to a bunch filling the rf bucket uniformly. Although the first maximum is $A \sim 0.2$, the actual ringing amplitude is roughly $B \approx 0.33$. It is easy to show that $I_1/(2I_0) = 1/3$. In other words, even when the bunch fills up the bucket, the beam loading voltage is decreased by a factor of only 3.

We plot in Fig. 8.15 $I_1/(2I_0)$ as functions of F, the total bunch length in units of rf wavelength, for various bunch distribution. We see that when the bunch is short, $I_1/(2I_0)$

drops very slowly with F and is distribution weakly-dependent only when the bunch is long. When the total bunch length equal the bucket length or $F = 1$, $I_1/(2I_0) = 1/2$, $\exp(-\pi^2/16)$, $1/3$, and $3/\pi^2$, respectively, for the cosine-square, Gaussian, cosine, and parabolic distribution.
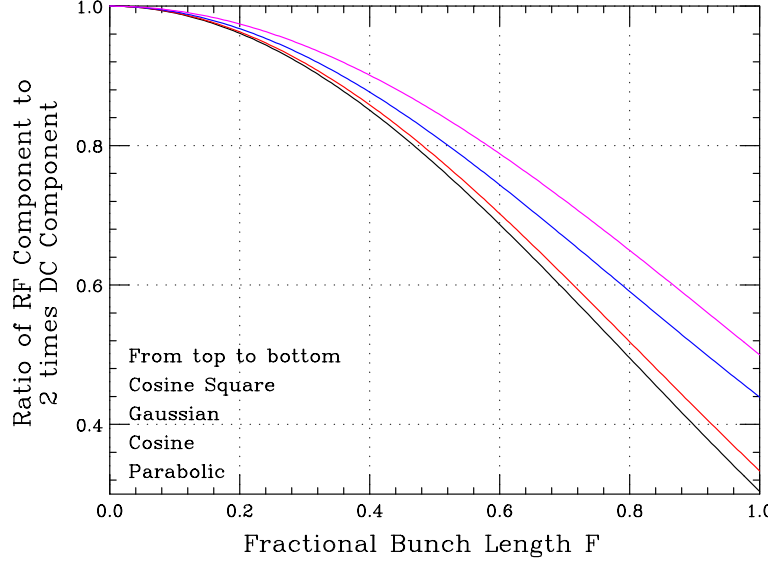

Figure 8.15: Ratio of the rf component of the bunch to two times the dc component, $I_1/(2I_0)$, as functions of F, total bunch length in units of bucket length, for, from top to bottom, cosine-square, Gaussian, cosine, and parabolic distributions.

8.4.4   Transient Compensation

We are going to give a short overview of some methods to cope with transient beam loading. The serious readers are referred to the references for further reading.

For a ring in the storage mode with all rf buckets filled with bunches of equal charges, each bunch is seeing exactly the same beam loading voltage, except for the influence of its small amount of synchrotron motion. We say that the beam loading is in the steady state and compensation can be made by detuning the cavity if the beam intensity is not too high.

However, the beam loading in many circumstances is in the transient state when there is a sudden change in beam intensity. One example is injection when bunches are

injected one by one. The beam loading voltage inside the rf cavity will increase linear with time, and the beam loading voltage seen by a bunch depends on time as well as its location along the ring. Obviously, slow extraction of an intense beam will also lead to sudden changes in the beam loading voltage. Another example is a gap left in an accelerator ring to allow for the firing of the injection and extraction kickers. Such a gap is also beneficial in clearing particles of opposite charge trapped inside the beam in order to eliminate collective two-stream instability. In the presence of a gap, the total beam loading voltage experienced in a cavity will be different during different bunch passages. For example, the bunch just after the gap will see the smallest beam loading voltage and the bunch just preceding the gap will see the most. As a result, the last bunch in the bunch train or batch will always see a lower rf voltage than the first bunch. At best, there will be a synchronous phase difference between the bunches leading to increase in longitudinal bunch area. At worst, the final bunches of the batch will not have enough voltage for stability. Strictly speaking, the word *transient* has been used wrongly for the problem of a gap, because such an effect occurs even when the stored beam is in the steady state. The uneven beam loading voltage experienced by the different bunches in the batch is a result of having many frequency components in the beam loading voltage besides the ones at the rf frequency and its multiples. Because of this, we should define the term *transient beam loading* as effects at frequencies other than the fundamental rf, its multiples, and their synchrotron sidebands.

One way to reduce beam loading, either steady-state or transient, is to reduce the loaded shunt impedance R_L of the cavity seen by the beam [9]. An obvious method is to add a resistance in parallel. Although this reduces the voltage created by both the beam and the power amplifier, however, the power requirements of the amplifier are increased. If the power amplifiers are already operating at their capacity, this is not an applicable solution.

Another possibility for reducing the beam loading voltage generated by the beam is to have another power amplifier to supply an additional generator current I_g equal and opposite to the beam image current. These two currents cancel each other at the cavity gap, making the cavity look like a short circuit to the beam. This method is very fast because there is no need to fight against the filling time of the cavity since there is no net current flowing across the cavity gap at all and therefore no additional fields created inside the cavity. This is a powerful but expensive solution due to the extra amplifier required. It is called high-level feed-forward compensation and is applicable for fixed rf frequency only. It was added to the CERN Intersecting Storage Ring (ISR)

rf system not so much to improve stability but due to a power limitation in the rf power amplifier. It can be shown [3] that the extra power required can become halved if the cavity is halfly pretuned before the injection so that the peak powers before and after injection are the same. In other words, the power is unmodulated even when the beam is fully modulated. The required power can be lowered by a factor of two again if there is optimum matching between the rf generator and the cavity. This can be accomplished by having a circulator inserted between the rf power and the cavity so that the additional current for the beam loading compensation means also real power.

To avoid high power consumption, there are also methods for low-level compensation. One technique is referred to as *feed-forward* [10]. The bunch current at a location preceding the cavity in the accelerator ring is measured and the signal is added to the low-level rf drive of the power amplifier so that an additional generator current I_g equal and opposite beam current is generated at the time the bunch crosses the cavity gap, as illustrated in Fig. 8.16. Experience and analysis show a dramatic increase in the
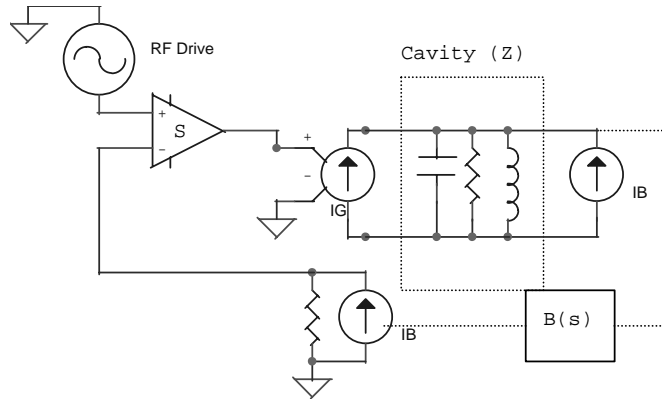

Figure 8.16: Block diagram of direct rf feed-forward, where $B(s)$ is the beam response and S is the transconductance of the amplifier.

instability threshold. This scheme has been successfully applied in the CERN Proton Synchrotron (PS) and the CERN Proton Synchrotron Booster (PSB). The instability threshold can probably be raised an order of magnitude. This is because the cavity voltage is completely decoupled from the beam signal, which nullifies the Robinson's instability. However, it is difficult to apply when the rf frequency is varying. The feedback path through the beam response is fairly weak, so the risk of creating an unstable system response is low. However, with a weak feedback, any errors in the system will not be compensated, so it is very important that the delay and phase advance of the

systems are properly tuned for beam cancellation. In practice, maintaining an error free system is very difficult when large amounts of impedance reduction is required.

A second technique of reducing the cavity impedance is amplifier feedback. The voltage in the cavity is measured, amplified and added to the low-level rf drive, as is illustrated in Fig. 8.17. To compute the impedance seen by the beam, the input at the
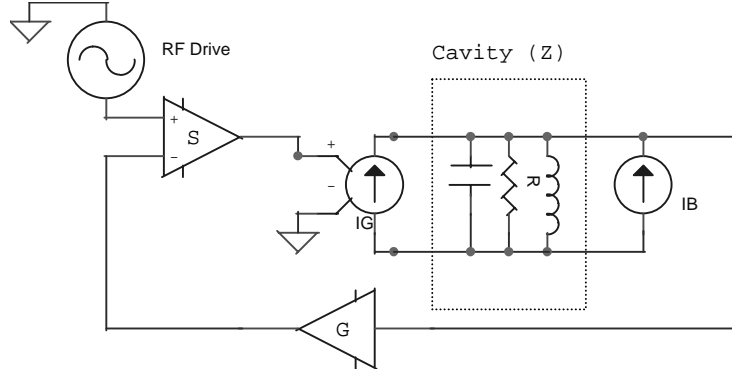

Figure 8.17: Block diagram of direct rf feedback, where the amplifier gain is G and the transconductance is S. The effective impedance seen by the beam is reduced from R_L to $R_L/(1 + SGR_L)$.

generator is turned off. The cavity voltage is amplified to $GV_{\rm rf}$ where G is the gain. It is then transformed into a current $-SGV_{\rm rf}$ through the transconductance S. This current is next fed through the generator and produces the additional gap voltage $-SGV_{\rm rf}Z$, giving a total gap voltage of $V_{\rm rf} = V_b - SGV_{\rm rf}Z$, where $V_b = R_L i_b$ is the beam loading voltage produced by the beam current i_b in the absence of the feedback loop. The effective impedance experienced by the beam becomes

$$R_{\rm eff} = \frac{R_L}{1 + SGR_L} \, , \tag{8.105}$$

where $H = SGR_L$ is called the open loop gain. Thus, by increasing the gain, the shunt impedance can be largely reduced. The main feedback path for this system no longer includes the beam response, and it is much stronger. The low-level feedback is very fast and the delay just depends on the length of the cables of the feedback loop. This is the most powerful method known and can be applied even for varying rf frequency. It has been applied to the CERN ISR at 9.5 MHz with $H = 60$, the CERN Antiproton Accumulator at 1.85 MHz with $H = 120$, and the CERN PSB at 6 to 16 MHz with $H = 5$ to 12.

In addition, there are a number of feedback loops in an rf accelerating system to assure that the particle beam will be accelerated according to the prescribed ramp design and to guarantee stability even when the Robinson's stability limit is exceeded. In the rf system of the former Fermilab Main Ring, for example, there are five feedback loops: [11]
(1) Rf frequency control loop, which compares the beam bunch phase versus rf phase comparitor and output an error signal. It is dc coupled with very low bandwidth. rf frequency.
(2) Beam radial position control loop, which controls the radial position of the beam by making small adjustment to the synchronous phase angle. It is dc coupled with bandwidth about 10 kHz.
(3) Correction loop for cavity gap voltage phase versus generator voltage phase. It is ac coupled with 5 MHz bandwidth and is capable of fast adjustment of cavity excitation phase to compensate for transient beam loading effects.
(4) Cavity voltage amplitude control loop, which adjusts the generator current such that the rf voltage amplitude developed at the cavity gap equals to its prescribed value. It has a very high dc gain (~ 60 db) and corner frequency 5 Hz.
(5) Detuning loop, which monitors the load angle between the generator current and the cavity gap voltage and adjusts the cavity tuning through ferrite biasing so that the load impedance presented to the generator appears to be real. It has a high dc gain (~ 60 db) with low bandwidth and corner frequency 1 Hz.
Among these, the second and third loops are the fastest, while the detuning loop is the slowest. These loops are not only limited by their gains, because they are only independent when the beam intensity is low. As the beam intensity increases, they become coupled and gradually lose their function.

For large rf systems, long delays may be unavoidable and the conventional rf feedback would have a too restricted bandwidth, may be much smaller than the cavity bandwidth itself. However, in the spectrum of transient beam loading, it is only those revolution harmonic lines that require nullification, and there is nothing in between the harmonics. With a return path transfer function having a comb-filter shape with maxima at every revolution harmonic, this condition can be satisfied. The overall delay of the system must be extended to exactly one machine turn to ensure the correct phase at the harmonics. Nullifying the beam signals at the revolution harmonics other than the fundamental rf frequency cures the transient beam loading.

8.4.4.1 Coupled-Bunch Instabilities

As will be discussed in Chapter 9, narrow resonances located at the synchrotron side-bands may excite longitudinal coupled-bunch instabilities. Although these narrow resonances originate mostly from the higher-order modes of the cavities, some may also comes from the revolution harmonics of the beam loading voltage excited because of having asymmetric fill in the stored beam. These harmonic lines have finite widths due to energy spread of the bunches and the synchrotron oscillations that develop because of the rf phase offsets. Thus, these harmonic components of the beam loading voltage can drive coupled-bunch instabilities and their nullification through comb-filter shape feedback is very essential.

Even for a ring of bunches with asymmetric gaps, the detuning of the cavities may also drive coupled bunch instabilities. This happens for a large machine where the revolution frequency f_0 is low. Detuning can very often shift the peak of the intrinsic resonant frequency of the cavities by more than one or more revolution harmonic. Here, we use a design of the former Superconducting Super Collider (SSC) as an example [5]. The average beam current is $I_0 = 0.073$ A. and a 374.7-MHz rf system is chosen. There are 8 cavities each having a shunt impedance $R_L = 2.01$ MΩ and $R_L/Q_L = 125$ Ω, or $Q_L = 1.608 \times 10^4$. At storage, the rf gap voltage per cavity is $V_{\rm rf} = 0.5$ MV. Thus the required detuning is given by

$$2Q_L \frac{\omega_r - \omega\text{rf}}{\omega_r} = \tan\psi = \frac{i_i m \cos\phi_s}{i_0} \ . \tag{8.106}$$

At $\phi_s \approx \pi$ and using short-bunch approximation, we obtain

$$\frac{\omega_r - \omega\text{rf}}{\omega_r} = -\frac{i_{\rm im} R_L}{2V_{\rm rf} Q_L} = -0.183 \times 10^{-4} \ , \tag{8.107}$$

or a detuning of $\Delta f_r = -6.84$ kHz. The half bandwidth of the loaded cavity is $\Delta f = f_r/(2Q_L) = 11.68$ kHz. However the revolution frequency of the collider ring is only $f_0 = 3.614$ kHz. In other words, the resonant impedance of the cavities would occur at a frequency slightly greater than $f_{\rm rf} - 2f_0$ and have a spread covering about 10 revolution harmonics. Such impedance could drive longitudinal coupled-bunch instabilities with considerable strength. If we compute this with the Fermilab Main Ring at a total of 3.25×10^{13} protons in the ring, we find that $|\Delta f_r/f_f| = 1.33 \times 10^{-4}$ or $|\Delta f_r| = 7.1$ kHz during acceleration, while the half bandwidth of the cavities is ~ 4.4 kHz. These numbers are very much less than the revolution frequency $f_0 = 47.7$ kHz. On the other hand, the

200-MHz traveling-wave accelerating structures in the CERN Super Proton Synchrotron (SPS) have a considerable bandwidth so that the impedance at $f_{\rm rf} \pm n f_0$ for small n is appreciable. Coupled-bunch instabilities arising from this impedance have been reported [6]. This also happens in the Low Energy Ring (LER) of the SLAC B-factory. Matching the klystron to the rf cavities requires the cavity be detuned to a frequency near $f_{\rm rf} - 1.5 f_0$, thus driving longitudinal coupled-bunch instabilities [7] in modes -1 and -2. Longitudinal coupled-bunch instabilities are usually alleviated by damping passively the driving resonances in the cavity or employing a mode damper. Here, the problem is quite different. First, we cannot damp this fundamental mode passively because we require it to supply energy to the beam. Second, usually the higher-order resonances that drive the coupled-bunch instabilities are much weaker than the fundamental. However, it is the fundamental that drives the coupled-bunch instabilities here. In other words, a very much powerful damper will be necessary to remove the instabilities. Because of this complication, a solution to this problem proposed in the SSC Conceptual Design Report is not to detune the cavity at the expense of increasing the required rf power.

8.5   Examples

8.5.1   Fermilab Main Ring

Once the former Fermilab Main Ring operated above transition in $M = 567$ consecutive bunches with total intensity 5×10^{13} protons. The ring consisted of $h = 1113$ rf buckets and the rf frequency was $\omega_r/(2\pi) = 53.09$ MHz There were 15 rf cavities, each of which had a loaded shunt impedance of $R_L = 500$ kΩ and the loaded quality factor was $Q_L = 5000$.

At steady state, the kth bunch in a bunch train of M bunches sees a beam loading voltage of (Exercise 8.7)

$$V_{bk} = V_0 e^{-(k-1)\delta_L} + V_{b0} \left(\tfrac{1}{2} + e^{-\delta_L} + \cdots + e^{-(k-1)\delta_L} \right) \ , \qquad (8.108)$$

where $\delta_L = \pi/Q_L$ is the decay decrement,

$$V_{b0} = \frac{qB\omega_r R_L}{Q_L} \qquad (8.109)$$

is the transient beam loading voltage left by a bunch carrying charge q, B is a parameter defined in Eq. (8.104) to take care of the fact that the bunch has a finite length, and is

equal to the current component at the rf frequency divided by twice the dc current, and

$$V_0 = V_{b0} \frac{e^{-(h-M+1)\delta_L} - e^{-h\delta_L}}{(1 - e^{-\delta_L})(1 - e^{-h\delta_L})} \tag{8.110}$$

is the beam loading voltage seen by the first bunch due to the excitation by earlier passages of the beam. The difference in beam loading voltage experienced by the last and the first bunch is therefore

$$\Delta V_b = V_{b0} \frac{e^{-\delta_L}[1 - e^{-(M-1)\delta_L}][1 - e^{-(h-M)\delta_L}]}{(1 - e^{-\delta_L})(1 - e^{-h\delta_L})} \ . \tag{8.111}$$

For the Fermilab Main Ring with $B = 0.872$, we obtain $V_{b0} = 0.411$ kV and $\Delta V_b = 113$ kV for one cavity. In the storage mode the gap voltage per cavity was $V_{rf} = 66$ kV. Thus, if the generator current I_g is in phase with the gap voltage and the synchronous angle was exactly $\phi_s = \pi$ at the passage of the first bunch through the cavity, the last bunch will see a synchronous angle $\phi_s = \tan^{-1}(\delta V_b/V_{rf}) \approx \frac{1}{3}\pi$. Such a large shift is intolerable because this will lead to a synchrotron oscillation of the center of the last bunch with an amplitude of $\frac{1}{6}\pi$ and finally result in a large growth of longitudinal emittance. There was a correction loop in the rf system that was capable of adding plus or minus quadrature currents up to $\sqrt{3}$ times the existing generator current to the input of the power amplifier [11]. With such an addition the synchronous angle goes back to π. The response time was ~ 300 ns, about 16 bunch periods, and was limited by the length of the cable loop. During such time, a maximum synchrotron phase shift of only $2.8°$ could develop and was tolerable.

Equation (8.111) shows that ΔV_b is small when there are only a small number of consecutive bunches in the ring ($M \to 1$). This is expected because it just gives the sum of the beam loading voltages of these few bunches while $V_0 \to 0$. On the other hand, if the ring is almost filled ($M \to h$), ΔV_b is also small, because of this is close to a symmetric filling of the ring. It is easy to show that the maximum ΔV_b occurs when the ring is half filled, or when the length of the gap is equal to the length of the bunch train.

8.5.2 Fermilab Booster

The injection into the Fermilab Booster from the Fermilab Linac is continuous for up to 10 Booster turns. After that the beam is bunched by adiabatic capture, which takes

place in about 150 μs while the rf voltage increases to 100 kV. During the injection, the beam is coasting and does not contain any component of the rf frequency. However, during adiabatic capture, both the rf voltage and the rf component of the current increase. If the former does not increase fast enough, Robinson's stability criterion will be violated. In general, the most dangerous moment is when the bucket area is equal to the bunch area. After that, the ratio of rf component beam signal to rf voltage decreases. However, the rf voltage during adiabatic capture in the Booster is maintained through counter-phasing. This is accomplished by dividing the 18 cavities into two groups. The required voltage amplitude and synchronous angle are obtained by varying the relative phase between the two groups. Thus the gap voltage in each cavity is not small and individually Robinson's stability is satisfied in each cavity. Counter-phasing is essential during adiabatic capture: First, maintaining too low a gap voltage inside a cavity will cause multi-pactoring. Second, the response of raising rf voltage during the capture through varying the generator current is slow because one has to fight the quality factor of the cavities, whereas controlling the rf voltage through varying the relative phase is fast. Since the beam loading voltage always points in the same direction aside from a detuning angle, to achieve counter-phasing, the generator current must be different in the two sets of cavities. The implication is that it will not be possible to have the generator current in phase with the gap voltage. Thus extra rf power will be required [12].

In the present booster cycle, the maximum power delivered to the beam is $P_b = 265$ kW at $V_{\text{rf}} = 864$ kV, while the maximum power lost to the ferrites is $P_L = 830$ kW. Since $P_b < P_L$ all the time, phase stability is guaranteed. To ensure that the beam accelerates according to the designed ramp curve, there is a slow low-level feedback loop which keeps the beam at the correct radial position in the aperture of the vacuum chamber by adjusting the synchronous phase angle. There is also a fast low-level feedback loop which damps phase oscillations. At extraction, since all bunches are kicked out at the same location in one revolution turn, the bunches will not see any transient beam loading voltage at all.

Actually, there are usually only $M = 80$ bunches in the ring of rf harmonic $h = 84$, and 4 bunch spaces are reserved for the extraction kicker. At the intensity of 6×10^{10} proton per bunch, the transient beam loading voltage excited in each of the 18 cavities by one bunch at passage is $V_{b0} = q\omega_r R_L/Q_L = 37.9$ V where $R_L/Q_L \sim 13$ Ω per cavity. According to Eq. (8.111), the difference in beam loading voltage experienced between the last and first bunch is $\Delta V_b = 3.76 V_{b0} = 142$ V. The beam gap is created near the end of the ramp, where the rf voltage has the lowest value of 305 kV at extraction, or

16.9 kV per cavity. This amounts to an rf phase error of 0.48°. Typically, a bunch at extraction has a half width of 2.8 ns or 54°. Thus the phase error is comparatively small and so is the increase in bunch area due to dilution. For this reason, no action is necessary to compensate for this gap-induced beam loading.

8.5.3   Fermilab Main Injector

A batch of 84 bunches is extracted from the Fermilab Booster and injected into the Fermilab Main Injector. The rf frequency is $\omega_r/(2\pi) = 52.8$ MHz and the rf harmonic is $h = 588$. Each bunch contains 6×10^{10} particles. At injection, at the rf voltage of 1.2 MV and a bunch area of 0.15 eV-s, the half length is 28.3 ns. There are 18 rf cavities with a total $R_L/Q_L = 1.872$ kΩ and $Q_L = 5000$. At the passage of the first bunch across the cavities, the transient beam loading voltage excited in all the cavities is $V_b = qB\omega_r R_L/Q_L = 5.46$ kV, where we have taken $B = 0.915$ by assuming a parabolic distribution. At the passage of the last bunch of the batch, the total beam loading voltage excited becomes $V_b = 444$ kV, where we have taken into account the decay decrement but the detuning has been set to zero. If there is a second batch transferred from the Booster, this will take place after one Booster cycle or 66.7 ms. During this time interval, steady-state has already reached, since the fill time of the cavities is $2Q_L/\omega_r = 30$ μs (about 2.7 turns). Figure 8.18 shows the beam loading voltages experienced by the 84 bunches in the batch in their first, second, and third passages through the cavities. The top trace represents the voltages seen when steady-state is reached. The difference in beam loading voltages seen by last and first bunch can be read out from the figure. It can also be computed analytically from Eq. (8.111) to be $\Delta V_b = 388$ kV. Actually, this difference is not much different from that experienced even in the first revolution turn because of the large quality factor of the cavities. The designed rf voltage at injection is $V_{\rm rf} = 1.2$ MV. If the designed synchronous phase $\phi_s = 0$ is synchronized to the middle bunch of the batch, the phase error introduced becomes $\Delta\phi_s = \pm 9.18°$ for the first and last bunches. This large difference in beam loading voltage, however, will not lead to energy difference along the bunches. The off-phase bunches will be driven into synchrotron motion instead. The first and last bunch will have amplitudes of oscillation $\Delta\phi_s = \pm 9.18°$. Eventually, the bunch area will increase. Measured in rf phase, the half width of the bunch at injection is 53.8°. Thus, the bunch length will increase linearly from the middle bunch towards the front and the rear of the batch, with a maximum fractional increase of 9.18/53.8=17%. Such an increase is tolerable at this moment. There is a fast feedback loop with a delay of only 16 bunch spacings (300 ns), implying
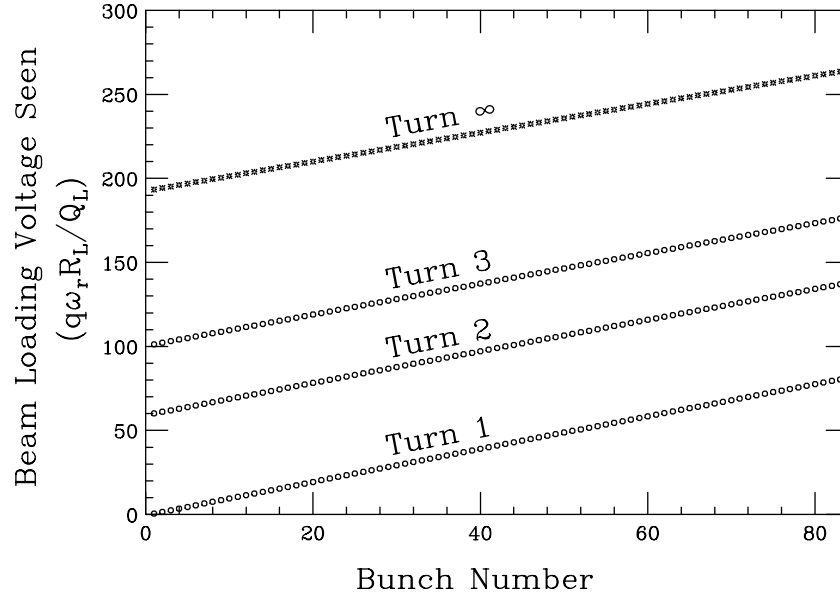
Figure 8.18: Beam loading voltages experienced by the 84 bunches in the batch at their first, second, and third passages of the Main Injector rf cavities. The top trace shows the beam loading voltages when steady state is reached. In the computation, cavity detuning has been set to zero.

that the maximum difference in beam loading voltage will only be ~ 88 kV and the phase error introduced will only be $\sim \pm 2.1°$. Unfortunately, this feedback loop is not working most of the time.

Notice that proper detuning does not help here if we want to keep the generator current in phase with the rf voltage for the middle bunch. For half of the batch (42 bunches), the accumulated phase shift due to detuning is of the order of $1°$ so that the transient beam loading voltages of individual bunches still add up almost in a straight line (Exercise 8.8).

There is an upgrade plan that increases the bunch intensity by a factor of 5. The transient beam loading will then become intolerable, because the phase error can be as large as $\Delta\phi_s = \pm 58°$. One proposal of compensation is feedforward. One proposal is to replace all the cavities with ones that have the same Q_L, but with R_L/Q_L reduced by a factor of 5. The beam loading effects will be the same as before. However, reducing the shunt impedance R_L 5 times implies the requirement of a larger generator current

($\sqrt{5} = 2.2$ times) in order to supply the same rf power.

There is a plan to slip-stack two Booster batches and capture them into 84 bunches of double intensity [8]. In order that two series of rf buckets can fit into the momentum aperture of the Main Injector, the rf voltage employed to sustain the bunches will have to decrease to less than 100 kV. Relatively, the transient beam loading problem becomes very severe. To control beam loading, the followings are planned:

1. Using only 2 or 4 of the 18 cavities to produce the required rf voltage and de-Qing the remaining cavities. One simple technique that may de-Q the cavities by a factor of 3 is to turn off the screen voltage to reduce the tube plate resistance.

2. Feed-forward the signal of the wall current monitored at a resistive-wall gap to the cavity drivers. Experience at the Main Ring expects to achieve a 10-fold reduction in the effective wall current flowing into the cavities.

3. Feedback on all the cavities. A signal proportional to the gap voltage is amplified, inverted, and applied to the driver amplifier. Based on experience in the Main Ring and results achieved elsewhere, a 100-fold reduction can be achieved.

8.5.4   Proposed Prebooster

Let us look into the design of a proposed Fermilab prebooster which has a circumference of 158.07 m. It accelerates 4 bunches each containing 0.25×10^{14} protons from the kinetic energy 1 to 3 GeV. Because of the high intensity of the beam, the problems of space charge and beam loading must be addressed. We wish to examine the issues of beam loading and Robinson instabilities based on a preliminary rf system proposed by Griffin [13].

8.5.4.1   The Ramp Curve

Because of the high beam intensity, the longitudinal space-charge impedance per harmonic is $Z_\parallel/n|_{\mathrm{spch}} \sim -j100\ \Omega$. But the beam pipe discontinuity will contribute only about $Z_\parallel/n|_{\mathrm{ind}} \sim j20\ \Omega$ of inductive impedance. The space-charge force will be a large fraction of the rf-cavity gap voltage that intends to focus the bunch. A proposal is to insert ferrite rings into the vacuum chamber to counteract this space-charge force [14]. An experiment of ferrite insertion was performed at the Los Alamos Proton Storage Ring and the result has been promising [15]. Here we assume such an insertion will
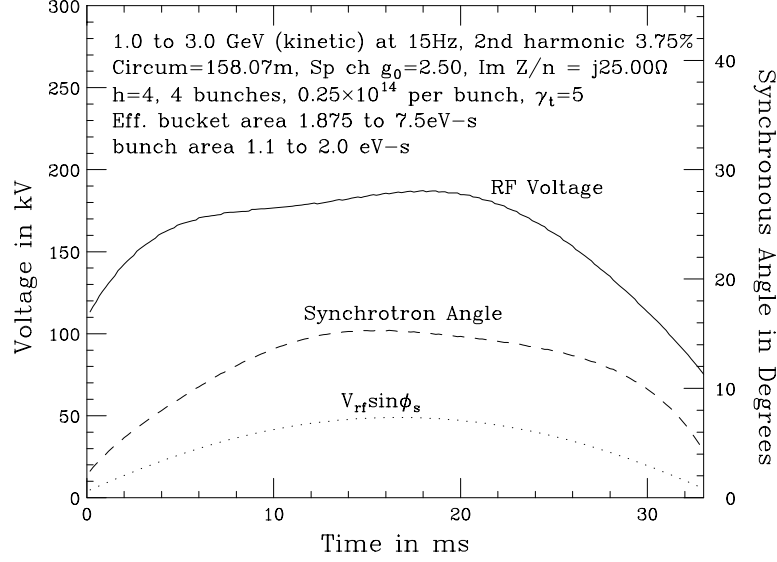
Figure 8.19: A typical ramp curve for a design of the future Fermilab prebooster.

over-compensate all the space-charge force leaving behind about $Z_\parallel/n|_{\text{ind}} \approx j25\ \Omega$ of inductive impedance. An over-compensation of the space charge will help bunching so that the required rf voltage needed will be smaller.

The acceleration from kinetic energy 1 to 3 GeV in 4 buckets at a repetition rate of 15 Hz is to be performed by resonant ramping. In order to reduce the maximum rf voltage required, about 3.75% of second harmonic is added. A typical ramp curve, with bucket area increasing quadratically with momentum, is shown in Fig. 8.19, which will be used as a reference for the analysis below. If the present choice of initial and final bucket areas and bunch areas is relaxed, the fraction of second harmonic can be increased. However, when the second harmonic is beyond $\sim 12.5\%$, it will only flatten the rf gap voltage in the ramp but will not decrease the maximum significantly.

8.5.4.2   The RF System

According to the ramp curve in Fig. 8.19, the peak voltage of the rf system is $V_{\text{rf}} \approx$ 185 kV. Griffin proposed 10 cavities [13], each delivering a maximum of 19.0 kV. Each cavity contains 26.8 cm of ferrite rings with inner and outer radii 20 and 35 cm, respectively. The ferrite has a relative magnetic permeability of $\mu_r = 21$. The inductance and capacitance of the cavity are $L \sim 0.630\ \mu\text{H}$ and $C \sim 820\ \text{pF}$. Assuming an average
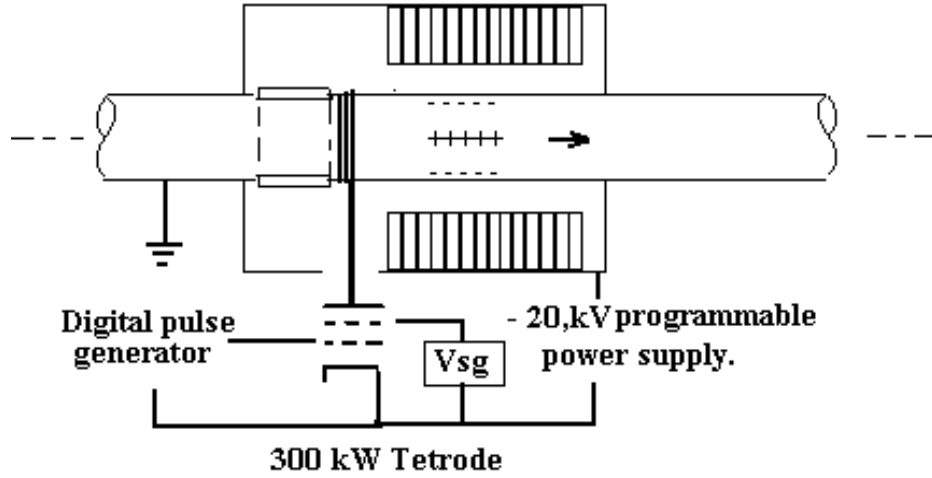
Figure 8.20: Transient beam loading power tetrode connected directly to an rf cavity gap to feed-forward the same amount of negative charge to the downstream end of the cavity gap so as to cancel the positive charge created there as the beam passes by.

ferrite loss of 134 kW/m^3, the dissipation in the ferrite and wall of the cavity will be $P \sim 14.2$ kW. The mean energy stored is $W \sim 0.15$ J. Therefore each cavity has a quality factor $Q \sim 459$ and a shunt impedance $R_s \sim 12.7$ kΩ.

Because each bunch contains $q = 4.005$ μC, the transient beam loading is large. For the passage of one bunch, 4.005 μC of positive charge will be left at downstream end of the cavity gap creating a transient beam loading voltage of $V_{b0} \sim q/C = 5.0$ kV, where $C = 820$ pF is the gap capacitance. We note from Fig. 8.19 that the accelerating gap voltages at both ends of the ramp are only about or less than 10 kV in each cavity. If the wakes due to the bunches ahead do not die out, we need to add up the contribution due to all previous bunch passages. Assuming a loaded quality factor of $Q_L = 45$, we find from Eq. (8.72) that the accumulated beam loading voltage can reach a magnitude of $V_b = 73$ kV when the detuning angle is zero (see Fig. 8.26).

A feed-forward system is suggested which will deliver via a tetrode the same amount of negative charge to the downstream end of the gap so as to cancel the positive charge created there as the beam passes by. Without the excess positive charge, there will not be any more transient beam loading. This is illustrated in Fig. 8.20.

Here, we are in a situation where the image current i_{im} passing through the cavity

gap is not equal to the beam current i_b. However, either at zero detuning or nonzero detuning, Eqs. (8.17) and (8.41) indicate that the portion of generator power transmitted to the acceleration of the beam is directly proportional to the magnitude of the image current. If the image current goes to zero in this feed-forward scheme, this implies that the rf generator is not delivering any power to the particle beam at all, although the beam is seeing an accelerating gap voltage. Then, how can the particle beam be accelerated? The answer is simple, the power comes from the tetrode that is doing the feed-forward. This explains why the tetrode has to be of high power.

Actually, the feed-forward system is not perfect and we assume that the cancellation is 85 %. For a δ-function beam, the component at the fundamental rf frequency is 56.0 A. Therefore, the remaining image current across the gap is $i_{\rm im} = 8.4$ A. To counter this remaining 15% of beam loading in the steady state, the cavity must be detuned according to Eq. (8.30) by the angle

$$\psi = \tan^{-1}\left(\frac{i_{\rm im}\cos\phi_s}{i_0}\right) \ , \tag{8.112}$$

where ϕ_s is the synchronous angle and $i_0 = V_{\rm rf}/R_s$ is the cavity current *in phase* with the cavity gap voltage $V_{\rm rf}$. For high quality factor of $Q = 459$ which is accompanied by a large shunt impedance, the detuning angle will be large. Corresponding to the ramp curve of Fig. 8.19, the detuning angle is plotted as dashes in Fig. 8.21 along with the synchronous angle and maximum cavity gap voltage. We see that the detuning angle is between 80° and 86°, which is too large. If a large driving tube is installed with anode (or cathode follower) dissipation at ~ 131 kW, the quality factor will be reduced to the loaded value of $Q_L \sim 45$ and the shunt impedance to the loaded value of $R_L \sim 1.38$ kΩ. The detuning angle then reduces to $\psi \sim 29°$ at the center of the ramp and to $\sim 40°$ or $\sim 56°$ at either end. This angle is also plotted in Fig. 8.21 as a dot-dashed curve for comparison. Then, this rf system becomes workable.

8.5.4.3   Fixed-Frequency RF Cavities

Now we want to raise the question whether it is possible to have a fixed resonant frequency for the cavity. A fixed-frequency cavity can be a very much simpler device because it may not need any biasing current at all. Thus the amount of cooling can be very much reduced and even unnecessary. It appears that the resonant frequency of the cavity should be chosen as the rf frequency at the *end* of the ramp, or $f_R = 7.37$ MHz so that the whole ramp will be immune to Robinson's phase-oscillation instability [4].
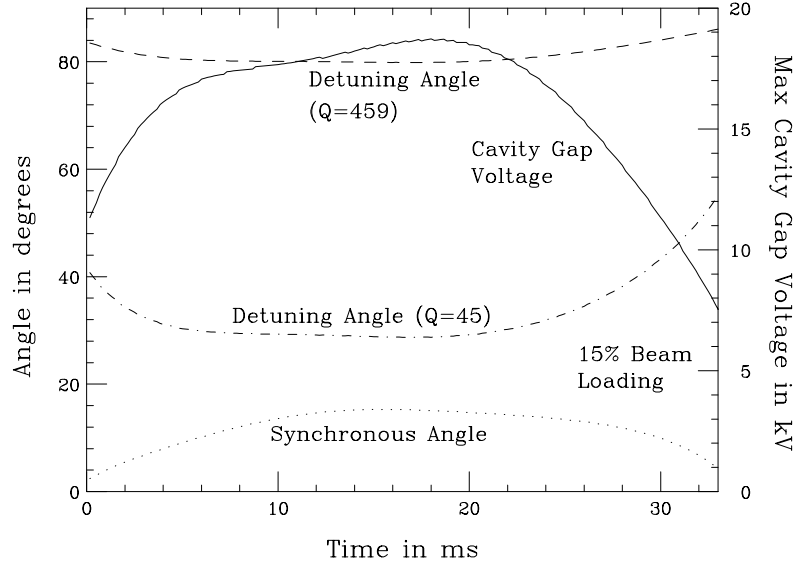
Figure 8.21: Detuning angle for the high $Q = 459$ and low $Q_L = 45$ situations.

However, the detuning will be large. For example, at the beginning of the ramp where $f_{\rm rf} = 6.64$ MHz, the detuning angle becomes $\psi = 85.2°$. Since the beam loading voltage $V_{\rm im}$ is small, the generator voltage phasor $\tilde{V}_g$ will be very close to the gap voltage phasor $\tilde{V}_{\rm rf}$. As a result, the angle θ between the gap voltage $\tilde{V}_{\rm rf}$ and the generator current phasor $\tilde{i}_g$ will be close to the detuning angle, as demonstrated in Fig. 8.22. For example, Fig. 8.23 shows that, at the beginning of the ramp, the detuning angle is $\psi = 85.2°$. Although the average total power delivered by the generator

$$\tfrac{1}{2}\tilde{i}_g \cdot \tilde{V}_{\rm rf} = \frac{V_{\rm rf}^2}{2R_L} + \tfrac{1}{2}i_{\rm im}V_{\rm rf}\cos\phi_s \tag{8.113}$$

is independent of θ, the energy capacity of the driving tube has to be very large.

Another alternative is to choose the resonant frequency of the cavity to be the rf frequency near the *middle* of the ramp. Then the detuning angle ψ and therefore the angle θ between $\tilde{V}_{\rm rf}$ and $\tilde{i}_g$ will be much smaller at the middle of the ramp when the gap voltage is large. Although θ will remain large at both ends of the ramp, however, this is not so important because the gap voltages are relatively smaller there. Figure 8.25 shows the scenario of setting the cavity resonating frequency f_R equal to $f_{\rm rf}$ at the ramp time of 13.33 ms.

There is a price to pay for this choice of f_R; namely, there will be Robinson phase instability for the second half of the ramp when the rf frequency is larger than f_R. The
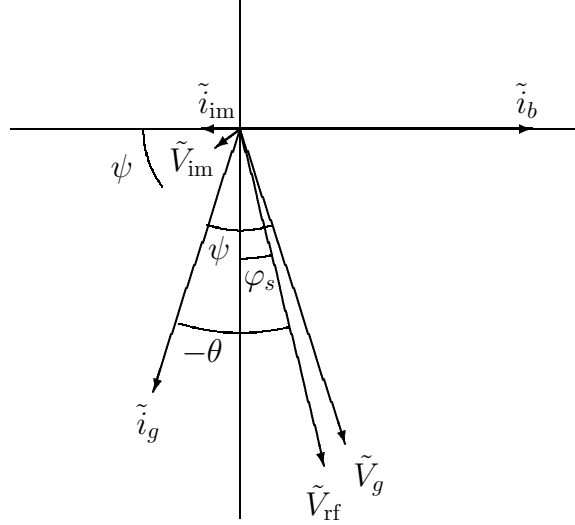
Figure 8.22: For a fixed cavity resonant frequency, the detuning angle ψ is fixed at each ramp time. When beam loading is small, the angle θ between the gap voltage $\tilde{V}_{\mathrm{rf}}$ and the generator current $\tilde{i}_g$ will be close to ψ and will be large.
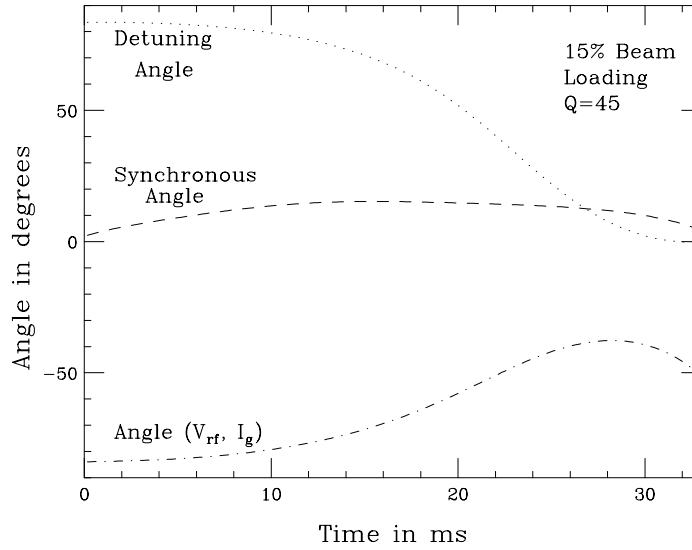

Figure 8.23: When the cavity resonant frequency is chosen as the rf frequency at the end of the ramp, both the detuning angle as well as the angle between the cavity gap voltage $\tilde{V}_{\mathrm{rf}}$ and the generator current $\tilde{I}_g$ are large.
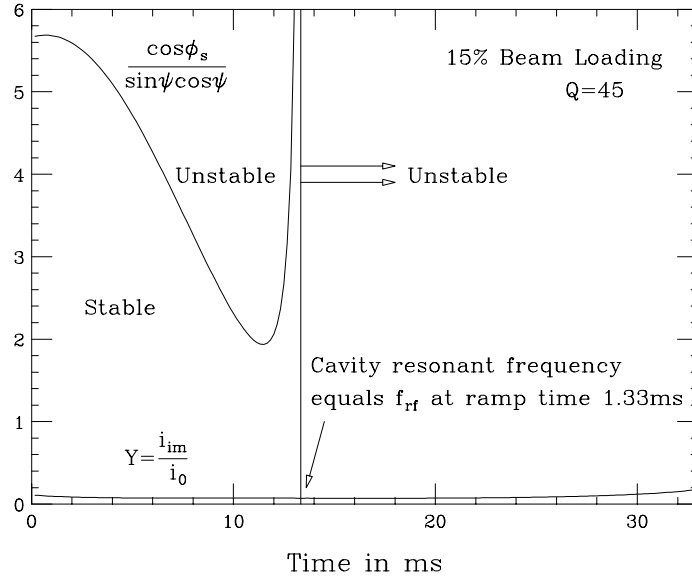
Figure 8.24: Plot showing the high-intensity Robinson's phase-stability criterion is satisfied in the first half of the ramp but not the second. Regions above the curve and to the left of the vertical straight line are unstable.
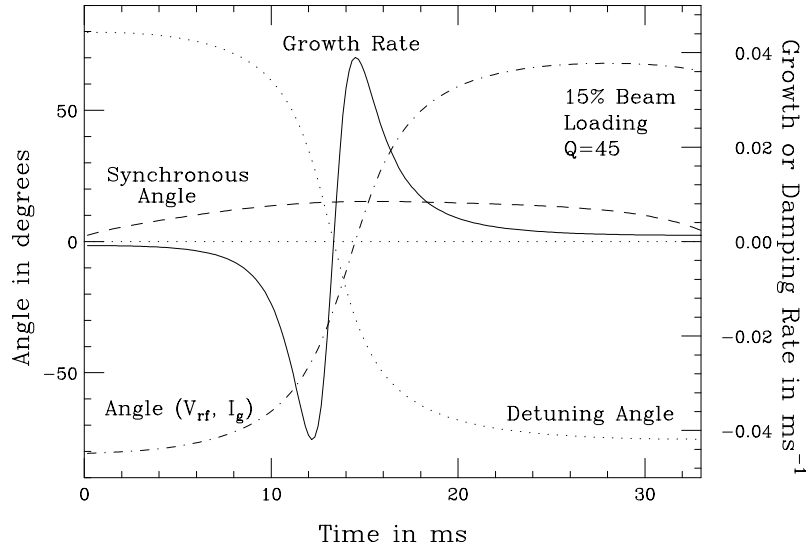

Figure 8.25: When the cavity resonant frequency is chosen as the rf frequency at the middle of the ramp at 13.33 ms, although the detuning angle as well as the angle between the cavity gap voltage $\tilde{V}_{\rm rf}$ and the generator current $\tilde{I}_g$ are large at both ends of the ramp, they are relatively smaller at the middle of the ramp where the gap voltage is large.

sufficient condition for having a potential well for stable oscillation is, from Eq. (8.47), the high-intensity Robinson's criterion:

$$\frac{V_{\text{br}}}{V_{\text{rf}}} < \frac{\cos\phi_s}{\sin\psi\cos\psi} \ , \tag{8.114}$$

where $V_{\text{br}} = i_{\text{im}}R_L$ is the in-phase beam loading voltage. Below transition, the synchronous angle ϕ_s is between 0 and $\frac{1}{2}\pi$. For the second half of the ramp, the rf frequency becomes higher than the resonant frequency of the cavity, we have $\psi < 0$. Figure 8.24 plots the criterion for the whole ramp. It shows that the criterion is well satisfied for the first half of the ramp but not satisfied for the second half. Therefore, we must rely on control loops in the rf system to maintain phase stability. Of course a low-level feedback loop to reduce the cavity impedance helps tremendously.

Even when the beam is in an potential well for oscillatory motion, we still need to worry whether the oscillation amplitude will grow or be damped. The instability comes from the fact that, below transition, the particles with larger energy have higher revolution frequency and see a smaller real impedance of the cavity, thus losing less energy than particles with smaller energy. Therefore, the synchrotron amplitude will grow. In other words, the upper synchrotron sideband of the image current interacts with a smaller real impedance of the cavity resonant peak than the lower synchrotron sideband. However, since the loaded quality factor Q_L is not small, the difference in real impedance at the two sidebands is only significant when the rf frequency is very close to the cavity resonant frequency. Thus, we expect the instability will last for only a very short time during the second half of the ramp. The growth rate of the synchrotron oscillation amplitude has been computed and is equal to [2]

$$\frac{1}{\tau} = -\frac{i_{\text{im}}\beta\omega_s(R_+ - R_-)}{2V_{\text{rf}}\cos\phi_s} \ , \tag{8.115}$$

where

$$R_+ - R_- = \mathcal{R}e\left[Z_{\text{cav}}(\omega_{\text{rf}}+\omega_s) - Z_{\text{cav}}(\omega_{\text{rf}}-\omega_s)\right] \ , \tag{8.116}$$

i_{im} is the image current, β is the velocity with respect to light velocity, $\omega_s/(2\pi)$ is the synchrotron frequency, and Z_{cav} is the longitudinal impedance of the cavity. We see from Fig. 8.25 that the growth occurs for only a few ms and the growth time is at least ~ 25 ms. The total integrated growth increment from ramp time 13.33 ms is $\Delta G = \int \tau^{-1}dt = 0.131$ and the total growth is $e^{\Delta G} - 1 = 14.0\%$ which is acceptable.

Finally let us compute the beam loading voltage seen by a bunch including all the effects of the previous bunch passage. In this example, $\delta_L \approx \pi h_b/Q_L = 0.0698$ for $h_b = 1$
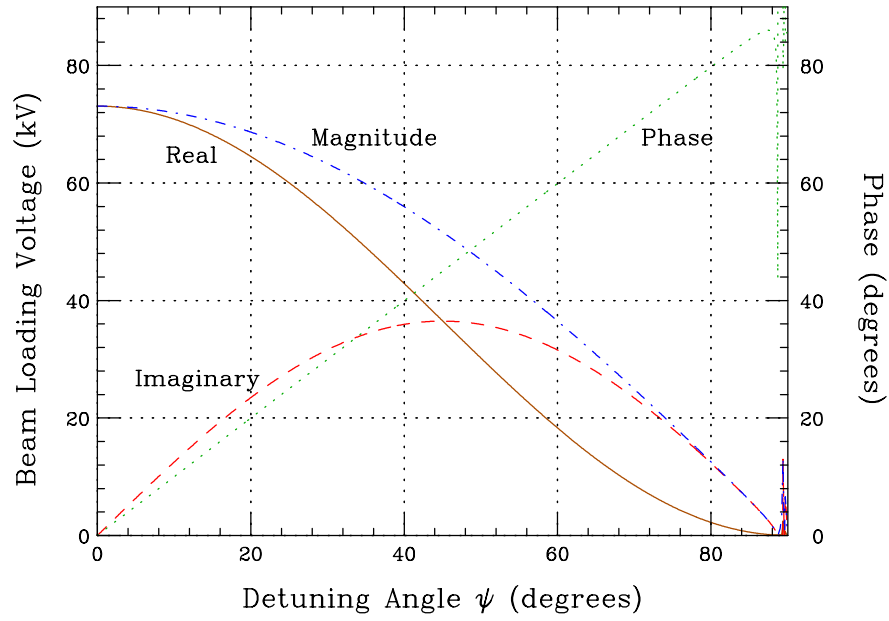
Figure 8.26: (color) Plot of transient beam loading voltage including all previous bunch passages, $\frac{q}{C}(F_1 + jF_2)$, versus detuning angle ψ.

Table 8.1: F_1 and F_2 for some values of the detuning angle ψ.

ψ	$\Psi = \delta_L \tan \psi$	F_1	F_2
$0°$	$0°$	$\sim \dfrac{1}{\delta_L}$	0
$84.9°$	$45°$	0.12	1.2
$87.5°$	$90°$	$\sim \dfrac{\delta_L}{2}$	$\sim \dfrac{1}{2}$
$88.7°$	$180°$	$\sim \dfrac{\delta_L}{4}$	0

and $Q_L = 45$. When the detuning angle $\psi = 0$, $V_b \approx V_{b0}/(2\delta_L)$. The functions F_1 and F_2 are computed at some other values of ψ, which are listed in Table 8.1 and plotted in Fig. 8.26. We see that the total transient beam loading voltage V_t falls rapidly as the detuning angle ψ increases. It vanishes approximately $\sim 88.7°$ and oscillates rapidly after that. However, the choice of a large ψ is not a good method to eliminate beam loading, because in general the angle between the generator current phasor $\tilde{i}_g$ and the rf voltage phasor $\tilde{V}_{\rm rf}$ will be large making the rf system inefficient.

8.6   Exercises

8.1. For a Gaussian bunch with rms length σ_τ in a storage ring, find the Fourier component of the current at the rf frequency. Give the condition under which this component is equal to twice the dc current.

8.2. Prove the fundamental theorem of beam loading when there are electromagnetic fields inside before the passage of any charged particle.

8.3. In Section 8.2, rf-detuning and Robinson's stability condition have been worked out below transition. Show that above transition the detuning according the Fig. 8.4 leads to instability. Draw a new phasor diagram for the situation above transition with stable rf-detuning. Rederive Robinson's high-intensity stability criterion above transition.

8.4. Derive Eq. (8.76), the generator power delivered to the rf system with multi-passage of equally spaced bunches.

8.5. (a) Derive Eq. (8.90), the beam loading voltage seen a charge particle inside a Gaussian bunch of rms length σ_τ at a distance τ ahead of the bunch center.
(b) Using the property of the complex error function,

$$
\lim_{\sigma_\tau \to 0} w\left(\frac{i\tau}{\sqrt{2}\sigma_\tau}\right) = \lim_{\sigma_\tau \to 0} \frac{2}{\sqrt{\pi}} e^{\tau^2/(2\sigma_\tau^2)} \int_{\frac{\tau}{\sqrt{2}\sigma_\tau}}^{\infty} e^{-t^2} dt = \left\{ \begin{array}{ll} 0 & \tau > 0 \ , \\ 1 & \tau = 0 \ , \\ 2 & \tau < 0 \ , \end{array} \right. \qquad (8.117)
$$

derive Eq. (8.92), the transient beam loading voltage seen by the head, center, and tail of the bunch as the bunch length shortens to zero.

8.6. (1) Derive Eqs. (8.94) and (8.95), the transient beam loading voltage seen by a charge particle in a bunch with parabolic distribution at a distance T from the head of the bunch.
(2) Derive Eqs. (8.99) and (8.99), the transient beam loading voltage seen by a charge particle in a bunch with cosine-square distribution at a distance T from the head of the bunch.
(3) Derive Eqs. (8.102) and (8.103), the transient beam loading voltage seen by a charge particle in a bunch with cosine distribution at a distance T from the head of the bunch.

8.7. For a batch with M consecutive bunches inside a ring of rf harmonic h, the steady-state beam loading voltage experienced by the kth bunch when it crosses the cavity gap is given by Eq. (8.5.1).
(1) Continuing bucket by bucket, write down the beam loading voltage experienced by the first bunch of the train when it crosses the cavity again. Since this beam loading voltage must equal to the one given by Eq. (8.5.1) with $k = 1$, determine the residual beam loading voltage V_0 in the cavity at that time and show that it is given by Eq. (8.110).
(2) Show that the difference in beam loading voltage ΔV_b experienced by the last and first bunch is given by Eq. (8.111).
(3) Show that ΔV_b assumes a maximum

$$\Delta V_b = V_{b0} \frac{e^{-\delta_L}\left[1 - e^{-\frac{1}{2}(h-1)\delta_L}\right]^2}{(1 - e^{-\delta_L})(1 - e^{-h\delta_L})} \ . \tag{8.118}$$

when $M = \frac{1}{2}(h + 1)$.

8.8. For a batch of 84 bunches inside the Fermilab Main Injector as described in Sec. 8.5.3,
(1) compute the detuning angle with the requirement that the generator current is in phase with the rf voltage with respect to the middle bunch of the batch,
(2) compute the rf phase slip between the transient beam loading voltages of successive bunches and show that because of the high quality factor the accumulation for half of the batch (42 bunches) is only around 1°.

8.9. Exercise 8.7 can also be pursued in the frequency domain. Fill in the missing steps of the following derivation.
(1) Consider $M = 2m$ point bunches each with charge q inside $M = 2m$ consecutive buckets in a ring with rf harmonic h. The current is

$$I(t) = q \sum_{n=1}^{m} \delta[t - (n - \tfrac{1}{2})T_b] + q \sum_{n=1}^{m} \delta[t + (n - \tfrac{1}{2})T_b] \ , \tag{8.119}$$

where T_b is the bucket width. In the frequency domain, the current at each revolution harmonic is given by

$$I_p = \frac{1}{T_0} \int_{-T_0/2}^{T_0/2} I(t)e^{-j2\pi pt/T_0} = \frac{2q}{T_0} \sum_{n=1}^{m} \cos\frac{2\pi p(n - \tfrac{1}{2})}{h} \ , \tag{8.120}$$

where $T_0 = hT_b$ is the revolution period and p is an integer ranging from $-\infty$ to $+\infty$.

(2) The beam loading voltage excited at each harmonic is $V_{bp} = I_p Z_p$ where the loaded impedance of the cavity is

$$Z_p = R_L \cos \psi_p e^{j\psi_p} \qquad \text{with} \qquad \tan \psi_p = 2Q_L \left(\frac{h}{p} - \frac{p}{h} \right) \ , \qquad (8.121)$$

and R_L and Q_L are the loaded shunt impedance and quality factor.

(3) Considering the symmetry of the impedance, the beam loading voltage in the time domain becomes

$$V_b(t) = \sum_p I_p \left(\cos^2 \phi_p \cos \frac{2\pi pt}{T_0} - \cos \phi_p \sin \psi_p \sin \frac{2\pi pt}{T_0} \right) \ . \qquad (8.122)$$

(4) Using the information of the Main Injector in Sec. 8.5.3, evaluate numerically and plot I_p, V_{bp}, and $V_b(t)$.

Bibliography

[1] P.B. Wilson, Fermilab Summer School, 1981, AIP Conference Proceedings, No. 87, 1982, AIP, p.450.

[2] See for example, H. Wiedemann, *Particle Accelerator Physics II*, Springer, 1995, p.203.

[3] D. Boussard, *Beam Loading*, Fifth Advanced CERN Accelerator Physics Course, Rhodes, Greece, Sep. 20-Oct. 1, 1993, CERN 95-06, p.415.

[4] P.B. Robinson, *Stability of Beam in Radiofrequency System*, Cambridge Electron Accel. Report CEAL-1010, 1964.

[5] E. Raka, *RF System Considerations for a Large Hadron Collider*, AIP Conference Proc. 184, Physics of Particle Accelerators, ed. M. Month and M. Dienes, AIP, New York, 1989, Vol. 1, p.289.

[6] D. Boussard et al., *Longitudinal Phenomena in the CERN SPS*, IEEE Trans. Nucl. Sc. **NS-24 No. 3**, 1399 (1977).

[7] *Conceptual Design Report of PEP-II, An Asymmetric B Factory*, June 1993, LBL-PUB-5379, SLAC-418, CALT-68-1869, UCRL-ID-114055, or UC-IIRPA-93-01.

[8] J. Dey, J. Steimel, J. Reid, *Narrowband Beam Loading Compensation in the Fermilab Main Injector Accelerating Cavities*, Proceedings of the 2001 Particle Accelerator Conference, Chicago, June 18-22, 2001, Ed. P. Lucas and S. Webber, p.876; Shekhar Shukla, John Marriner, and James Griffin, *Slip Stacking in the Fermilab Main Injector*, Proceedings of the Summer Study on the Future of High Energy Physics, Snowmass, July 1-20, 2001.

[9] J. Steimel, *Summary of RF Cavity Beam Loading Problems and Cures in the CERN PS Complex*, unpublished; D. Boussard and G. Lambert, *Reduction of the Apparent Impedance of Wide Band Accelerating Cavities by RF Feedback*, IEEE Trans. Nucl. Sc. **NS-30 No. 4**, 2239 (1983); D. Boussard, *Control of Cavities with High Beam Loading*, IEEE Trans. Nucl. Sc. **NS-32 No. 5**, 1852 (1985); D. Boussard, *RF Power Requirements for a High Intensity Proton Collider (Parts 1 and 2)*, CERN SL/91-16 (RFS), April 1991.

[10] F. Pedersen, *Beam Loading Effects in the CERN PS Booster*, IEEE Trans. Nucl. Sc. **NS-22 No. 3**, 1906 (1975); F. Pedersen, *A Novel RF Cavity Tuning Feedback Scheme for Heavy Beam Loading*, IEEE Trans. Nucl. Sc. **NS-32 No. 5**, 2138 (1985).

[11] J.E. Griffin, *Compensation for Beam Loading in the 400-GeV Fermilab Main Accelerator*, IEEE Trans. Nucl. Sc. **NS-22 No. 3**, 1910 (1975); D. Wildman, *Transient Beam Loading Compensation in the Fermilab Main Ring*, IEEE Trans. Nucl. Sc. **NS-32 No. 5**, 1910 (1985).

[12] Y. Goren and T.F. Wang, *Voltage Counter-Phasing in the SSC Low Energy Booster*, Proceedings of the 1993 Particle Accelerator Conference, May 17-20, 1993, Washington, DC, p. 883.

[13] J.E. Griffin, *RF System Considerations for a Muon Collider Proton Driver Synchrotrons*, Fermilab report FN-669, 1998.

[14] K.Y. Ng and Z.B. Qian, Proc. Phys. at the First Muon Collider and at Front End of a Muon Collider, Fermilab, Batavia, Nov. 6-9, 1997.

[15] J.E. Griffin, K.Y. Ng, Z.B. Qian, and D. Wildman, *Experimental Study of Passive Compensation of Space Charge Potential Well Distortion at the Los Alamos National Laboratory Proton Storage Ring*, Fermilab Report FN-661, 1997.